Bed Topography Inferred from Airborne Radio-Echo Sounding of Columbia Glacier, Alaska

U.S. GEOLOGICAL SURVEY PROFESSIONAL PAPER 1258–G

Front Cover: U.S. Geological Survey photograph No. 81R3–083 by Austin Post, September 26, 1981.

Bed Topography Inferred from Airborne Radio-Echo Sounding of Columbia Glacier, Alaska

By C. S. BROWN, L. A. RASMUSSEN, *and* M. F. MEIER

STUDIES OF COLUMBIA GLACIER, ALASKA

U.S. GEOLOGICAL SURVEY PROFESSIONAL PAPER 1258–G

UNITED STATES GOVERNMENT PRINTING OFFICE, WASHINGTON : 1986

DEPARTMENT OF THE INTERIOR

DONALD PAUL HODEL, *Secretary*

U.S. GEOLOGICAL SURVEY

Dallas L. Peck, *Director*

Library of Congress Cataloging-in-Publication Data

Brown, C S.
Bed topography inferred from airborne radio-echo sounding of Columbia Glacier, Alaska.

(Studies of Columbia Glacier, Alaska) (Geological Survey professional paper ; 1258–G)
Bibliography: p. G24
Supt. of Docs. no.: I 19.16:1258–G
1. Columbia Glacier (Alaska) 2. Echo sounding. 3. Radar in glaciology. I. Rasmussen, L.A. II. Meier, Mark Frederick, 1925– . III. Title. IV. Series. V. Series: Geological Survey professional paper ; 1258.
GB2427.C64B76 1986 551.3′12′097983 85–600300

For sale by the Books and Open-File Reports Section, U.S. Geological Survey,
Federal Center, Box 25425, Denver, CO 80225

CONTENTS

ILLUSTRATIONS

TABLE

SYMBOLS AND ABBREVIATIONS

Symbol	Name	Unit
c	Speed of light in air	300 m/μs
H	Airplane altitude above glacier surface	m
km	Kilometer.	
m	Meter.	
mm	Millimeter.	
MHz	Megahertz.	
n	Index of refraction of ice	dimensionless
q	Length of ice-segment of ray	m
R	Radius of curvature of reflection locus	m
r	Length of air-segment of ray	m
s	Second.	
μs	Microsecond.	
t	Time	μs
t_b	Arrival time for echo from glacier bed	μs
t_s	Arrival time for echo from glacier surface	μs
u	Horizontal distance from airplane position to refraction point	m
x	Horizontal coordinate, positive to east	m
y	Horizontal coordinate, positive to north	m
z	Vertical coordinate, positive upward	m
α, β, γ	Coefficients of plane locally approximating glacier surface	dimensionless
ϕ	Inclination of ice-ray from the vertical	degrees
θ	Inclination of air-ray from the vertical	degrees

BED TOPOGRAPHY INFERRED FROM AIRBORNE RADIO-ECHO SOUNDING OF COLUMBIA GLACIER, ALASKA

By C S. BROWN, L.A. RASMUSSEN, and M.F. MEIER

ABSTRACT

The first airborne radio-echo sounding of a temperate glacier was performed in 1978 at Columbia Glacier, a large (1,100-square-kilometer), grounded, iceberg-calving glacier 38 kilometers west of Valdez, Alaska. The sounding system used a low frequency (about 1.5 megahertz) to overcome scatterings from water-filled voids in the ice, a short pulse, and an untuned receiver. Transverse and longitudinal profiles were flown over the lower 7 kilometers of the glacier. The received signal, the horizontal position of the airplane, and its altitude above the glacier surface were recorded by an FM tape recorder. For the data analysis, pictures of received energy from each flight profile were reconstructed from the taped data using an oscilloscope. Use of intersecting profiles allowed an internal consistency check to determine whether the correct bed reflection had been chosen. A three-dimensional geometric method of determining the envelope of the reflection lobes was developed for interpreting the data, instead of the differential method used by previous investigators. This analysis provided bedrock altitude determinations at every node of a 200-meter square grid. The probable error in the inferred bed altitudes was estimated to be 30 meters; the greatest depth was 370 meters below sea level.

INTRODUCTION

Columbia Glacier (fig. 1) is a large, grounded, calving glacier near Valdez, Alaska, the terminus of the trans-Alaska pipeline. In 1978 it was 66.6 km long and 1,100 km^2 in area. Many large tributaries coalesce to form the lower trunk of the glacier, which fills a deep fiord and ends in a grounded, calving terminus that stands up to 90 m above sea level. From the time of the first recorded observation in 1794 (Vancouver, 1798) until 1978, the terminus had been relatively stable, ending partly on Heather Island (fig. 2) and partly on a submerged moraine shoal in water less than 100 m deep. Upglacier from the terminus, however, the bed is nearly 400 m below sea level.

Nearly all grounded, iceberg-calving glaciers in Alaska, such as Columbia Glacier, have experienced large-scale, asynchronous advances and retreats; Columbia Glacier, however, was the only glacier that extended in 1978 to its neoglacial moraine. The large-scale advances and retreats of calving glaciers are due not solely to climatic variations; water depth at the terminus is a critical factor. When a glacier retreats into a deep basin or fiord, instability results and the calving flux increases (Post, 1975; W.O. Field, oral commun., 1980; Brown and others, 1982).

In 1974, Columbia Glacier appeared to be entering a period of retreat (Post, 1975; Sikonia and Post, 1980). Since 1977, the U.S. Geological Survey has documented an accelerated rate of thinning in the terminus region and a trend of increasingly larger embayments forming, as an even greater portion of the terminus retreats from the crest of the shoal each summer and fall. Once the glacier has backed off the moraine shoal into the deep water upglacier, rapid and irreversible retreat is expected to begin. In October of 1984, all of the terminus was 1–2 km behind the shoal in water averaging 120 m deep; all evidence indicates that the large-scale recession has begun.

A direct consequence of rapid retreat is an increasing flux of icebergs. Even prior to 1974, small icebergs from the glacier drifted toward and occasionally into the shipping lanes in Valdez Arm (Kollmeyer and others, 1977); these shipping lanes are used by tankers transporting oil from the Alaska pipeline terminal at Valdez.

To determine when this rapid retreat might begin, and by how much the iceberg discharge might be increased, an intensive study was begun by the Geological Survey in 1977 (Meier and others, 1978). A prediction was made (Meier and others, 1980) that the glacier would begin an irreversible retreat within a few years. Details of each phase of this study are being published as a series of scientific papers, of which this is one. The other papers discuss the relationship of calving speed to water depth and other variables (Brown and others, 1982); surface topography (Rasmussen and Meier,

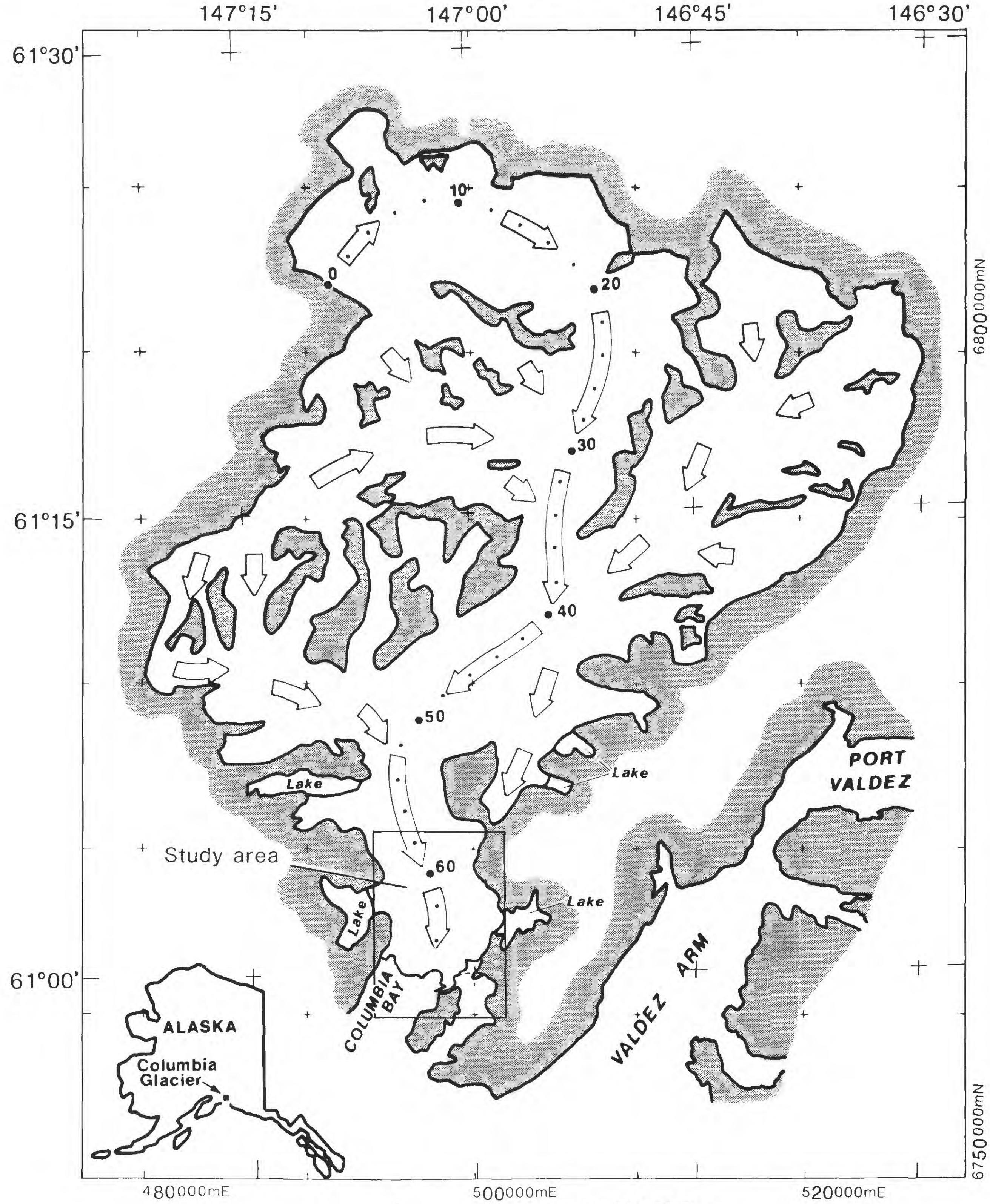

FIGURE 1.—Index map of Columbia Glacier, Alaska. Arrows indicate direction of ice flow. Main ice stream is indicated by longer arrows and dots at 2-kilometer intervals along the longitudinal coordinate system. Boxed area is region with inferred bed topography from the airborne radio-echo sounding.

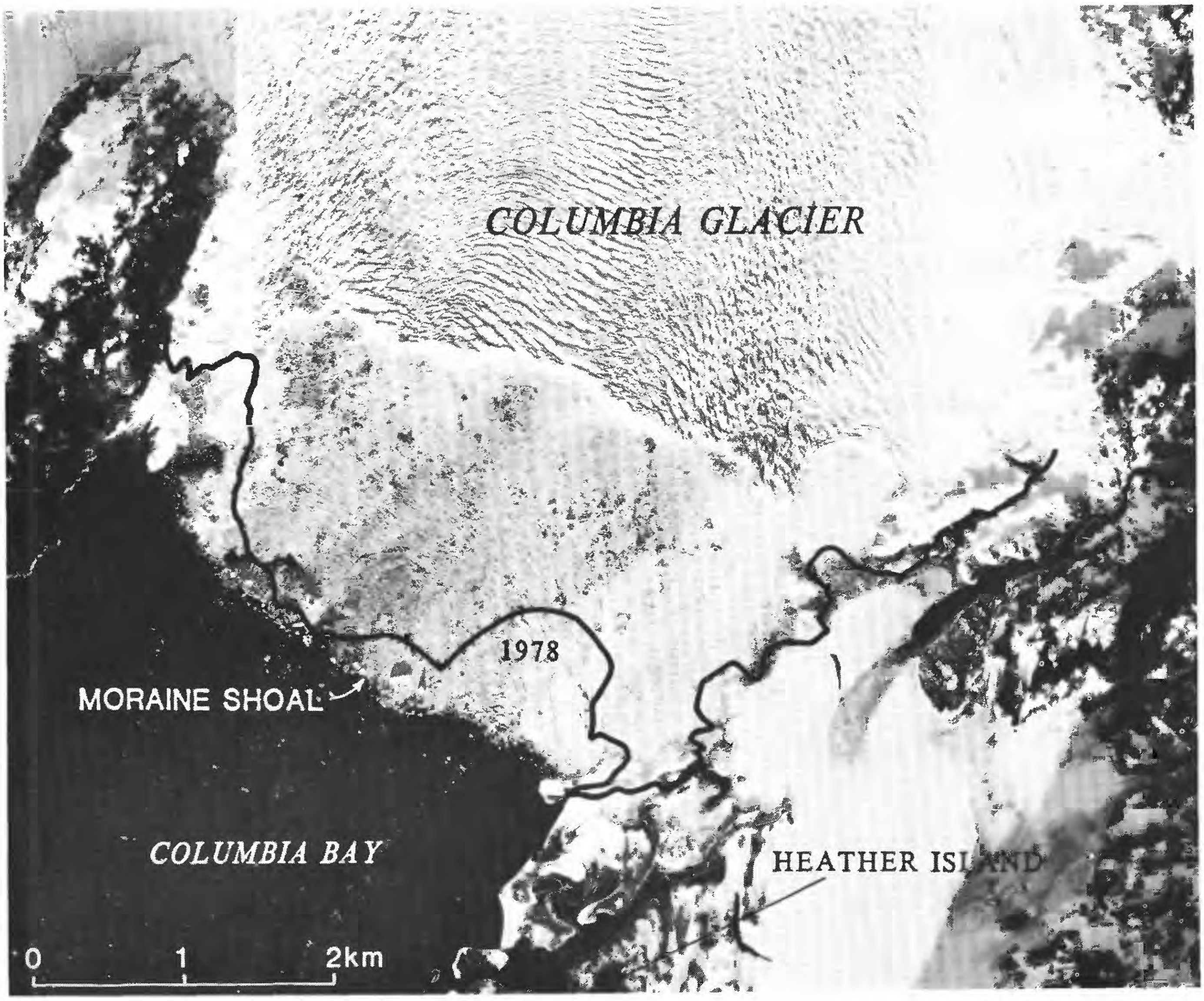

FIGURE 2.—Vertical aerial photograph of the terminus of Columbia Glacier, December 14, 1984. Also indicated is the position of the terminus on August 26, 1978, and the position of the moraine shoal.

1985); mass balance observations; field measurements of velocity, thickness, and thickness change (Mayo and others, 1979); photogrammetric determination of surface altitude, terminus position, and ice velocity (Fountain, 1982; Meier and others, 1985); the development of a data set that satisfies the continuity equation; the adjustment of velocity data to obey continuity (Rasmussen, 1985); a continuity model of the terminus retreat and the rate of iceberg discharge (Rasmussen and Meier, 1982); finite-element (Sikonia, 1982) and finite-difference (Bindschadler and Rasmussen, 1983) models of the flow of the lower glacier, which also predict iceberg flux; and several additional topics.

Glacier thickness is a principal variable in the equation of continuity, in the flow law, and in calving relationships; thus, it is crucial in any dynamic glacier model, such as those developed for predicting the behavior of Columbia Glacier. Thickness cannot easily be measured directly; drilling in the lower reach of Columbia Glacier is expensive, relatively slow, and prohibitively dangerous (fig. 3). Thickness, however, can be determined indirectly from the rather easily measured surface topography and an estimated bed topography. Currently, polar ice bodies are sounded by radio-echo methods. When it became necessary to know the thickness of Columbia Glacier, efforts to sound this

FIGURE 3.—Oblique aerial photograph showing the roughness of the Columbia Glacier surface. View is to the west, about 2 kilometers above the terminus. Average relief from summits to valleys is about 25 meters; local relief may range up to 40–50 meters. USGS photograph by M.F. Meier, August 14, 1984.

large, temperate glacier were begun. This was a formidable task, as radio-echo sounding techniques of temperate (nonpolar) ice bodies are relatively new and are still very much in the developmental stage. This paper outlines the development of radio-echo sounding methods for temperate glaciers, describes the collection and analyses of data in this first airborne radio-echo sounding of a temperate glacier, and explains how the bed topography, and thus the glacier thickness, were inferred from these data.

RADIO-ECHO SOUNDING DEVELOPMENT

Measurements of glacier thickness by radio methods were first attempted with some success in 1927 and 1928 (Evans, 1963c). Since the first reported radio sounding of polar ice in Antarctica in 1957 (Evans, 1963a), sounding of polar ice bodies by radio-echo methods has continued in Greenland and Antarctica (see, for instance, Evans, 1963b, 1967; Swithinbank, 1968; Robin and others, 1970; Morgan and Budd, 1975) and elsewhere. Recently, much emphasis has been placed on the interpretation of these returns (see, for instance, Harrison, 1970; Oswald, 1975; and Robin, 1975).

Research in applying radio-echo sounding methods to temperate glaciers first had to address the problems of sounding ice at the melting temperature, ice that is less homogeneous than polar ice. Smith and Evans (1972) determined that the difficulty of sounding temperate glaciers was due not to the high temperature, impurity content, or ice fabric but to the masking of the true bottom return by the diffuse return from the englacial scatterers, or inhomogeneities. Shortly thereafter, Watts and England (1976) correctly attributed these inhomogeneities to water-filled voids in the ice, determined that frequencies less than 10 MHz were needed to overcome the scatterings, and suggested that a short-pulse radar with an untuned receiver could be used at these low frequencies. This system differs from radars typically used for polar ice, which employ a modulated carrier signal and a tuned radio receiver. Vickers and Bollen (1974) introduced the technology of resistively loaded antennas, from which there is practically no reflection from the ends of the arms, to the radio-echo sounding of temperate glaciers. With this system, they successfully sounded depths of more than 200 m on South Cascade Glacier, a temperate glacier in the North Cascade Mountains of Washington, using 5 MHz frequency and then applied the system to Columbia Glacier (Vickers and Bollen, 1974). Since then, scientists at the University of Iceland developed a profiling system based on these principles, employing frequencies of 2 to 10 MHz, and used it successfully on the Vatnajökull and Mýrdalsjökull icecaps (Ferrari and others, 1976; Björnsson and others, 1977; Sverrison and others, 1978; Bishop and others, 1979; Björnsson, 1982). The system was towed behind a motorized sled and was the first successful attempt at continuous profiling on the surface of a temperate glacier.

THE AIRBORNE RADIO-ECHO SOUNDING SYSTEM

DEVELOPMENT OF THE SYSTEM

Sounding work was begun on Columbia Glacier during the summer of 1974 (Vickers and Bollen, 1974), when approximately 70 surface radar and gravimetric spot measurements were made, all in the lower 30 km of the main trunk glacier. For the purposes of numerical modeling, however, data from a much denser network of points were necessary. A continuous profiling system could not be operated on the glacier surface because of the many locations rendered inaccessible by the highly crevassed surface (fig. 3).

On the basis of successful sounding of South Cascade and Columbia Glaciers with a surface system, Watts and Wright (1981) designed an airborne radio-echo sounding system for use at Columbia Glacier, and used this system during August and September 1978. This was the first airborne radio-echo sounding of a temperate glacier. Owing to the severe time constraint under which the system was developed and flown, many problems involving data acquisition and analysis remained unsolved.

Data were obtained from 12 east-west and 7 north-south profiles covering the lower 7 km of the glacier (fig. 4), which is the most important region for studying the glacier flow. The airborne radar system was carried in a Fairchild-Pilatus Porter[1], a short-takeoff-and-landing airplane sufficiently large and powerful to carry all the equipment and personnel required and capable of flying at speeds low enough for radar work, around 100 knots (kn; 185 kilometers per hour (km/hr)).

Watts and Wright (1981) modified their surface monopulse generator for the airborne work; they were able to use transmitting and receiving antennas similar in principle to those used in the surface system but modified because they had to be fed in the center, yet could be attached to the airplane only at the ends. Because of these modifications and the proximity of the metal airplane, the emitted wave train contained about six cycles instead of the more desirable single sinusoid (Churchill and Wright, 1978).

An oscilloscope on board the airplane sampled the received signal and transformed it to an audio frequency that was recorded on a seven-track FM tape recorder. The oscilloscope also provided an output, recorded on another channel, that gave an absolute time correlation between echoes and their delay from the initial transmitted pulse. Photographs (fig. 5) were then taken of an oscilloscope composite reconstruction made by playing back the magnetic tapes. Time delay from the original transmitted pulse is plotted vertically, and the horizontal position represents movement above the surface; brightness was modulated in proportion to received (echo) voltage.

AIRPLANE POSITIONING

The horizontal position of the airplane was recorded in the local x,y coordinate system devised for Columbia Glacier which is related to the geodetic UTM (Universal Transverse Mercator) system according to

$$\begin{pmatrix} x \\ y \end{pmatrix} = \frac{1}{0.9996} \begin{pmatrix} \text{UTM Easting—490 km} \\ \text{UTM Northing—6,750 km} \end{pmatrix} \qquad (1)$$

The x,y position was determined by an automated navigation system using two microwave transponders located at known points off the edge of the glacier. It measured the times of the responses from the transponders, and a small computer on the airplane then calculated the position. The distances to the transponders, and thus the x,y position, were recorded every 0.5 s.

[1]The use of brand names in this report is for identification purposes only and does not imply endorsement by the U.S. Geological Survey.

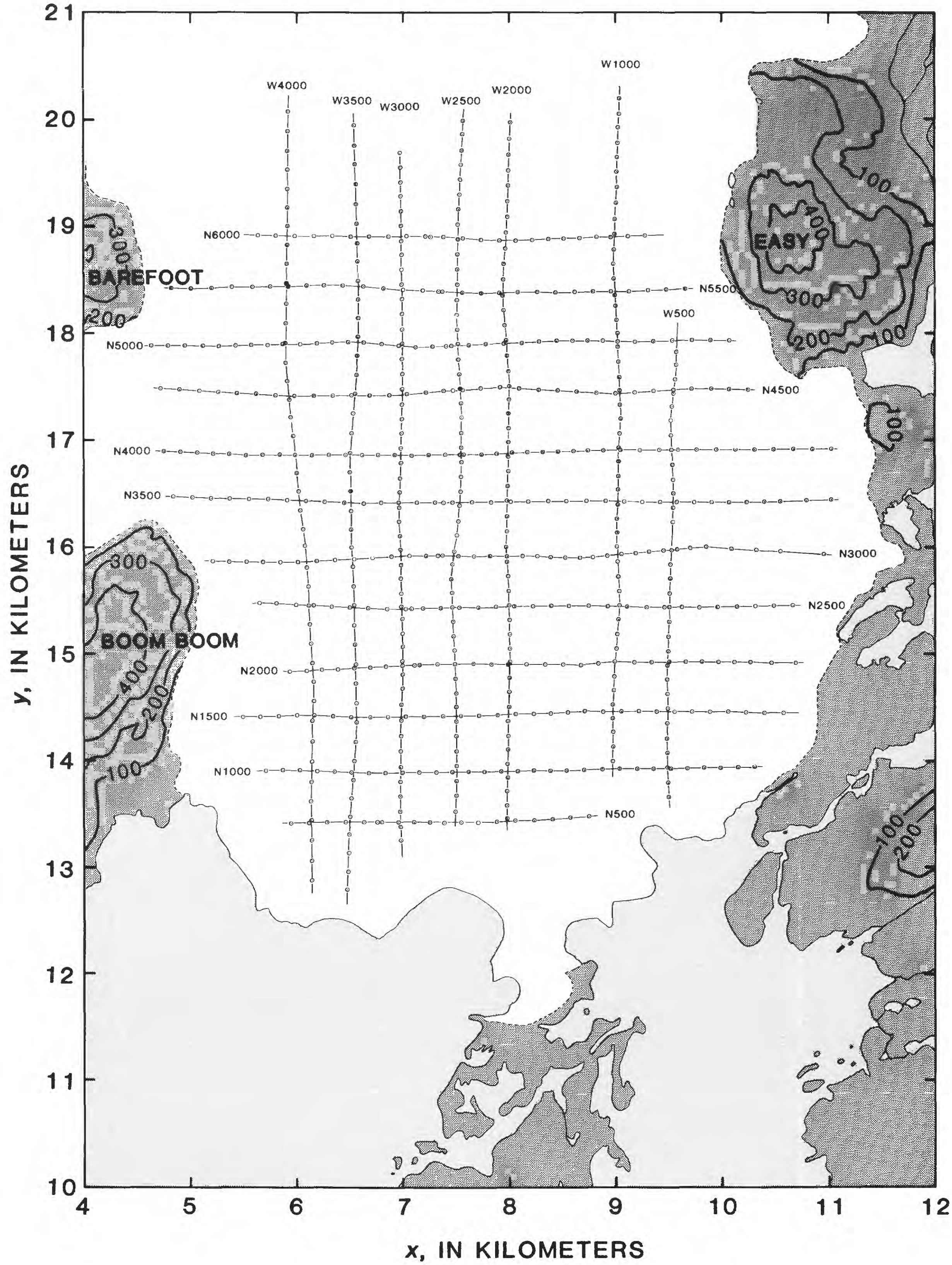

FIGURE 4.—Flight paths and sounding positions from which the Columbia Glacier bed topography was inferred. Dots represent the sounding positions; their location corresponds to the point where the echo arrival times t_b were read off the reconstructed profiles at approximately 5-millimeter intervals. If the maximum value of t_b did not occur at one of these roughly equally spaced positions, its position was also included. Note the close proximity of the Boom Boom, Barefoot, and Easy ridges; contours are given in meters above sea level. The location of the region depicted is indicated by the box in figure 1.

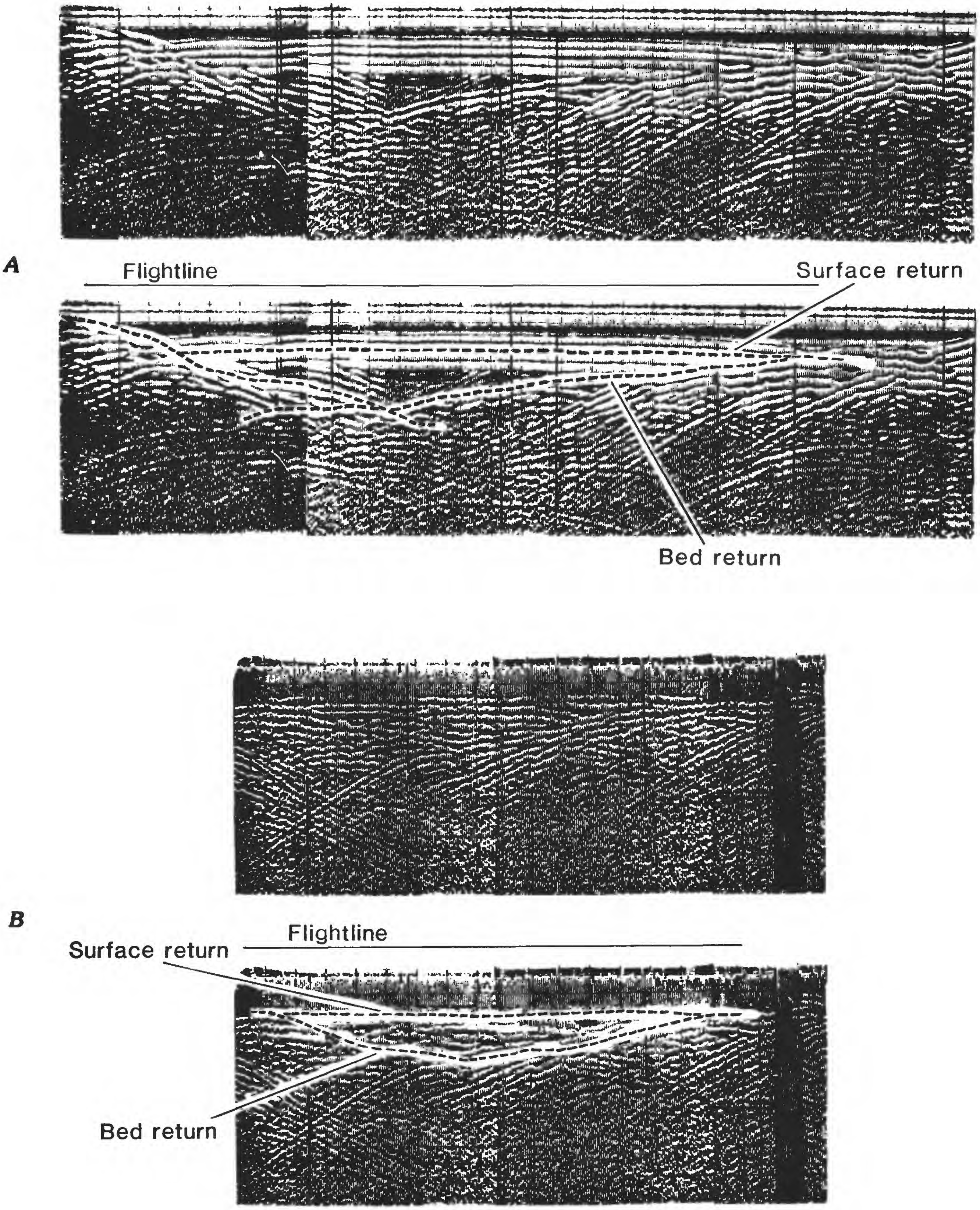

FIGURE 5.—Reconstructed airborne radio-echo profiles across the lower part of Columbia Glacier: (A) profile at y=14.4 kilometers, illustrating a reasonably good return; (B) profile at y=12.9 kilometers, illustrating a poor return and the difficulties in determining t_b. Each profile is shown twice, once with and once without the surface return and the selected bed return identified.

Twelve east-west profiles and seven north-south profiles were flown (fig. 4). The east-west profiles are termed the "North family," owing to their northward progression at 500-m increments from their baseline, and the north-south profiles are similarly termed the "West family."

The airplane's radar altimeter reading was also recorded every 0.5 s, giving H, the altitude in meters above the glacier surface. This was the only altitude recorded on the tape. The altitude at which the airplane was to fly each profile was predetermined and logged prior to flight; this was the barometric altitude to the nearest 100 ft (30 m). The horizontal distance along the flight path from the beginning of each profile was also recorded for use in locating the photographed arrival times in real space.

DATA ANALYSIS

SIGNAL EXTRACTION

The value of $t_b\,(x, y, z)$, the round-trip signal time to the bed from a particular airplane position, was measured manually from a photograph of an oscilloscope reconstruction of the profile. Figure 5 shows the reconstruction of both a good profile and a poor one; most were somewhere in between in quality. Obviously there were several difficulties to overcome before t_b could be measured. First was the problem of correlating the several bands (cycles) of the reflection with those of the transmitted pulse. Not only were there multiple bands, but each usually was not continuous across the profile. Sophisticated off-line signal processing could be used to compress these multiple bands, making it easier to distinguish the bottom echo. There also was the problem of the valley wall echoes masking returns from the glacier bed, particularly on the west edge of the glacier against the Boom Boom and Barefoot ridges (fig. 4). These valley wall returns likewise could have been removed by signal processing or eliminated at the outset by flying much closer to the glacier surface.

Owing to the electronic saturation of the airborne receiving system by the transmitted pulse, no echoes could be detected during the first several microseconds. Thus, variations in t_s were recorded but the absolute arrival time t_s of the echo from the surface was not recorded and the t-datum line, commonly referred to as the flightline, does not appear on the reconstructed profile pictures (the lines at the very top of the pictures are the tail end of the recovery from the saturation of the electronics). This flightline is necessary to measuring t_b, and reconstructing it was difficult. To approximate its position on the picture, the surface reflection corresponding to the selected bed return first had to be determined. In many cases there was not a one-to-one correspondence between the several surface bands and the several bands from the bed return. Usually the brightest and widest band was chosen; from the internal consistency check (below) it could be determined whether the corresponding bed reflection had been chosen correctly. Two points then were plotted, one at each end of the profile above the selected surface band at a distance corresponding to the average altitude of the airplane above the surface. This distance was determined by knowing the number of microseconds per division on the oscilloscope and by knowing the signal speed in air. A line drawn between these points was used as the t-datum line. The error in using this t-datum line was determined to be well within the 30-m error in airplane altitude H.

INTERNAL CONSISTENCY

The final phase of the data reduction was checking for internal consistency by comparing the two t_b values at each intersection of two profiles. Each t_b value was adjusted to account for possible differences in altitude at which the two profiles were flown. This was done by reducing each t_b by t_H, the amount of time for the airwave to travel the distance H:

$$t' \equiv t_b - t_H = t_b - 2H/c \quad , \tag{2}$$

in which $c = 300$ m/µs is the signal speed in air. The difference $|t'_N - t'_W|$ between the reduced t_b values for the east-west profile and the north-south profile was calculated for each of the 80 profile intersections. Although this formulation embodies the strict assumption that the echo comes from the nadir, the difference $|t'_N - t'_W|$ is little affected if the echo comes from elsewhere, so long as the echoes sensed on the two profiles come from approximately the same location. That is, the difference between the two nadir distances to the glacier surface is used to approximate the difference between the two slant distances actually traversed by the signal. Because the difference in H was generally small compared with H (fig. 6), this weaker assumption seems reasonable. As the error in measuring t_b on the photograph was a maximum of 0.45 µs, this value was used as the maximum allowable difference value of $|t'_N - t'_W|$. Sixty-three percent of the differences were actually less than 0.20 µs. One difference was 0.46 µs, for which there was no obvious explanation.

Matching t'_N and t'_W at each intersection provided a check for consistency between profiles. To check for consistency within a single profile, the band chosen as representing the bed reflection on the photograph from which one t_b was obtained had to be the same band used to measure the t_b values of the neighboring intersection points on the profile. At 5 (out of 138) profile intersec-

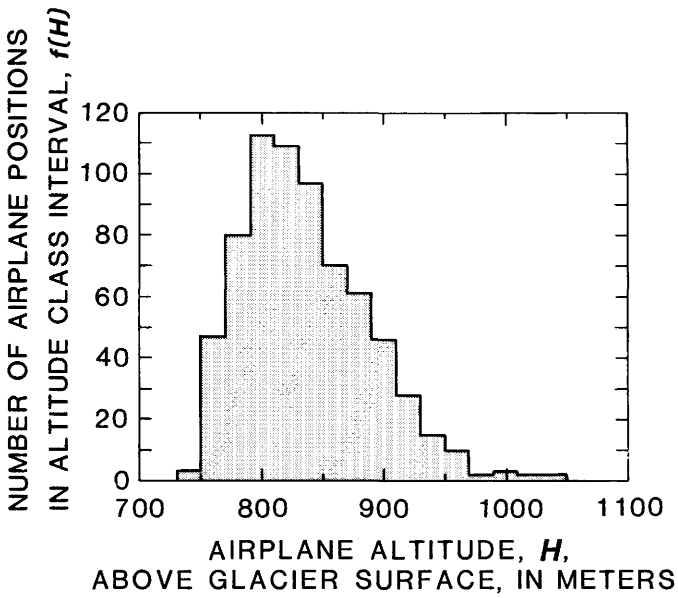

FIGURE 6.—Frequency distribution of altitude H of the airplane above the glacier surface. Shown are the number $f(H)$ of the 678 airplane positions within each of the indicated 20-meter-wide altitude intervals.

tions, it was necessary to choose a band different from the neighboring intersection. There is no definitive explanation for this; numerous factors undetected in the oscilloscope plot affect the reflected waveform. Once again, signal processing would probably yield more consistent results by virtue of putting almost all the energy into a single band.

Apparent internal consistency would result if every t_b in every profile were misinterpreted in the same way. The good agreement between the t_b values and both the directly measured bathymetry and the radar soundings from the surface makes this unlikely.

ERROR IN ECHO ARRIVAL TIMES

Although there were difficulties involving both the data acquisition and the data analysis, there were only two major sources of error. The first was in the altitude used to position the t-datum line on the photographs of the reconstructed profiles. This altitude was the barometric altitude rounded to the nearest 100 ft (30 m) at which it was predetermined the airplane should fly. It was referred to as the "average profile altitude," measured above mean sea level. It is assumed that the instrumental and reading error in altitude values during flight is of the order of 10 m, to which must be added the effect due to atmospheric pressure fluctuations, perhaps another 10 m. Therefore the aggregate error in flying the predetermined altitude is assumed to be about 30 m. Thus, at any given point on a profile and, therefore, in the t-datum line, there was an error of ± 30 m in the altitude value used. This corresponds to ± 0.20 μs on the photograph.

The second major source of error was in measuring t_b on the photographs. The bands chosen as representing the bed reflections on the profiles averaged 1 mm in width. Thus, this was the average amount by which the distance from the t-datum line to the chosen reflection could vary. By using the predetermined number of microseconds per division on the oscilloscope and the reduction factor between the oscilloscope screen and the photograph, the conversion factor on the photograph was calculated to be 0.30 μs/mm (microseconds per millimeter). Thus the 1 mm variation in measuring t_b corresponds to 0.30 μs. The possible inaccuracy in measuring t_b on the photograph was less than 0.3 mm (0.09 μs) and is considered to be negligible in relation to the other, much larger errors.

Instrumental errors, including those in the radio-echo sounder, oscilloscope, and the transponders used to determine the x,y position of the airplane, were deemed to be insignificant compared with the other errors. Thus, if the two sources of error are considered to be independent, the error in t_b is $[(0.20\ \mu s)^2 + (0.30\ \mu s)^2]^{1/2} = 0.36\ \mu s$. This error results directly in error in glacier thickness; however, as will be shown, the two are not strictly proportional. If the echo is assumed to come from the nadir, then 0.36 μs corresponds to 30 m.

INTERPRETATION OF AIRBORNE RADIO-ECHO SOUNDING DATA

The interpretation of the radio-echo sounding data is based on simple, known geometric principles, which are briefly reviewed here. Although they are ultimately applied three-dimensionally, they are initially described in two dimensions for ease of presentation. The simplicity of the mathematical model follows from several assumptions concerning the physics of the signal propagation and of the composition of the glacier, as well as recognition of the low quality of the original data.

Signal strength is assumed to be unreliably known, so that echo arrival time is the only variable used in inferring the distance traveled by the signal. The signal is assumed to be omnidirectional, so that no direction is ruled out as a candidate from which an echo may be received. Because of the uncertainty with which arrival times t_b were read from the reconstructed profiles, a simple geometric method of determining the envelope of the reflection lobes was selected for interpreting the data instead of the differential method used by Harrison (1970), which is based on the rate of change of the signal arrival time as the airplane moves along its flight path. The signal is assumed to travel in air at the rate of $c=300$ m/μs (meters per microsecond); within the glacier it is $1/n$ times this rate, where $n=1.78$ is taken to be the index of refraction of ice.

Although the glacier surface is highly irregular and fractured (fig. 3), the mathematical model assumes a much smoother, average surface at which refraction follows Snell's law (fig. 7):

$$\sin \phi = \frac{1}{n} \sin \theta \ . \qquad (3)$$

In fact, it assumes a piecewise planar surface between given altitudes on the nodes of a 200-m square grid. These were obtained by applying the method of optimum interpolation to photogrammetrically determined altitudes of irregularly positioned points appearing on a sequence of vertical aerial photographs

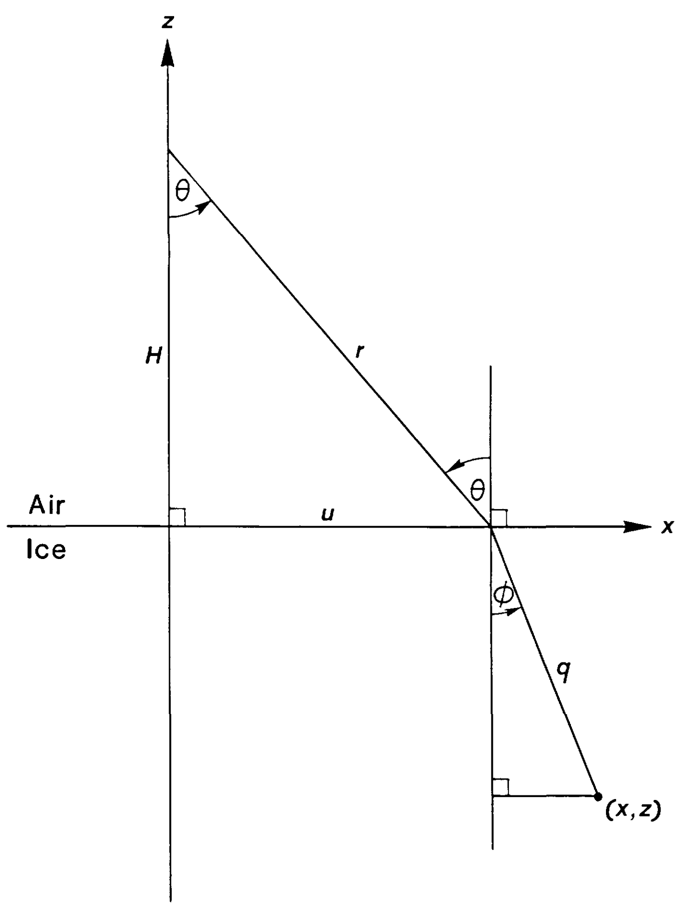

FIGURE 7.—A ray refracted according to Snell's law (equation 3).

taken on August 26, 1978, from about 6,800 m above the glacier surface (Rasmussen and Meier, 1985). This surface topography is represented in figure 8 by a manual contouring of the altitudes on the 200-m square grid. Because the soundings were taken in late August over the part of Columbia Glacier having surface altitudes less than 300 m above sea level, no correction—such as that used by Harrison (1970)—was applied to the passage of the signal through a firn layer, which would have an n-value smaller than that for ice. Another assumption that is made is that the arrival times that are used are from echoes occurring only at the glacier bed, rather than from englacial bodies of liquid phase water.

Change of airplane position during the period between signal transmission and reception is neglected. The 100-kn airplane speed (Watts and Wright, 1981) produces only 1 mm of displacement in 20 μs, a time that exceeds all signal arrival times obtained over Columbia Glacier. The 1 s consumed by the sampling oscilloscope in constructing a complete sweep (R.D. Watts, written commun., 1985) corresponds to a displacement of about 50 m.

REFRACTION AND REFLECTION REPRESENTED IN TWO DIMENSIONS

The dependence of the ice angle ϕ on the air angle θ that arises from using $n=1.78$ in equation 3 is shown in figure 9. This relationship gives a maximum value of $\phi=34.18°$ when $\theta=90°$, and the slope $d\phi/d\theta$ decreases continuously from $1/n$ at $\theta=0°$, to 0 at $\theta=90°$.

The distance equation for an echo with arrival time t_b is

$$ct_b = 2\ (r+nq)\ , \qquad (4)$$

in which r is the length of the air leg and q is the length of the ice leg (fig. 7). It is easily shown that the ray that obeys Snell's law is the one that minimizes the travel time between (x,z) and $(0,H)$.

A parametric representation of the x,z locus is easily obtained from equations 3 and 4 in terms of θ:

$$\left.\begin{aligned} x &= \frac{1}{n^2}\left[\frac{(n^2-1)H}{\cos\theta}+\frac{ct_b}{2}\right]\sin\theta \\ z &= \frac{1}{n^2}\left[\frac{H}{\cos\theta}-\frac{ct_b}{2}\right](n^2-\sin^2\theta)^{1/2} \end{aligned}\right\} \qquad (5)$$

This formulation is valid only for an idealized glacier surface lacking curvature. Although it is not possible here to give a closed-form expression $z=f(x)$ for the locus, equations 5 may easily be transformed so that

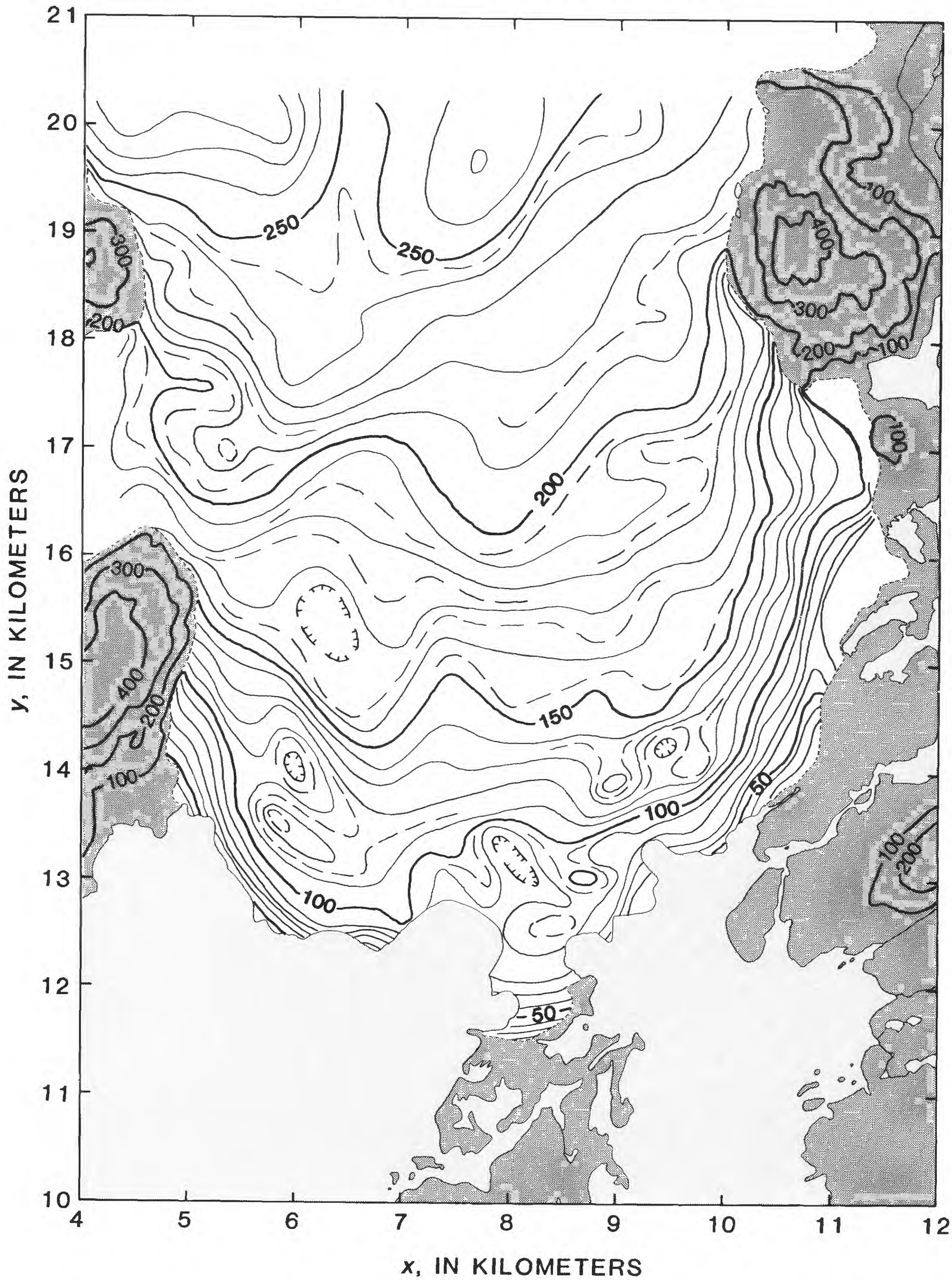

FIGURE 8.—Surface topography of lower part of Columbia Glacier on August 26, 1978. The location of this region is indicated by the box in figure 1. The contour interval on the glacier is 10 meters, with occasional 5-meter dashed contours. Datum is sea level.

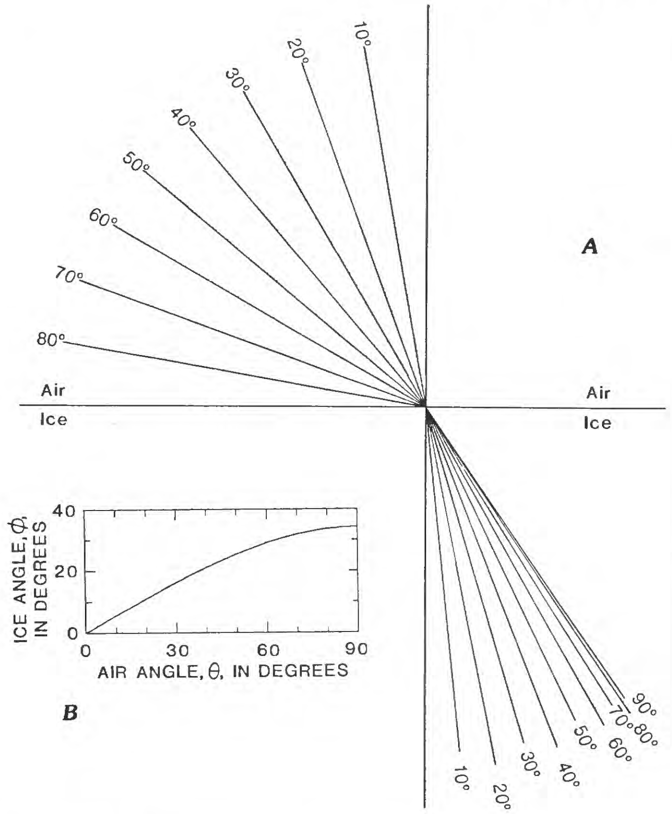

FIGURE 9.—Refraction according to Snell's law at the air-ice boundary for $n=1.78$ in the ice: (*A*) Specimen refracted rays. The ice ray and the air ray are both identified by the incidence angle θ of the air ray, as measured from the vertical. (*B*) Ice angle ϕ as a function of the air angle θ. The slope $d\phi/d\theta$ decreases continuously from $1/n$ at $\theta=0$ to 0 at $\theta=90°$ (where $\phi=34.18°$).

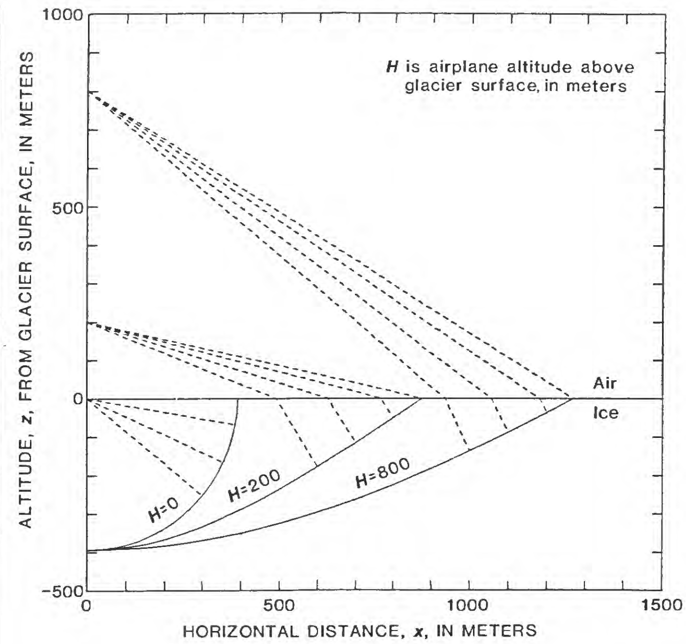

FIGURE 10.—Reflection loci for two soundings from above the glacier surface and for one from the surface itself. For each locus (solid curve), a few generating rays (dashed line) are shown. For the two soundings from above the surface, the rays refract at the surface according to Snell's law (eq. 3, fig. 9). A horizontal glacier surface is assumed; the complete reflection locus in three dimensions is actually the body of revolution obtained by rotating the locus about the z-axis.

the parameter is r or u or the locus slope dz/dx. Half of each of the x,z loci for three different airplane altitudes $H=0$, 200, and 800 m is shown in figure 10; all three loci are scaled to have the same $z=-393$ m depth (corresponding to $t_b=10$ μs when $H=800$ m, which is typical of the Columbia Glacier data) at $x=0$. The $H=0$ locus is constructed on the assumption that the antennas are in dielectric contact with the ice and, therefore, that no refraction occurs.

The x,z curve is strictly just a locus, in the sense that any point on it could be the source of the echo having the arrival time that determines the curve. If several loci were available from closely spaced airplane positions, then a glacier bed could be inferred from their envelope. No part of the bed can be above the envelope because, for one or more of the observation positions, an echo would have been received with an earlier arrival time than the one from which the locus was constructed. Several such loci, and a bed profile that is consistent with them but that is not uniquely determined by them, are shown in figure 11. Any other curve that was tangent to each of the several loci, and that nowhere rose above their envelope, might also be the bed profile.

Glaciological and geological knowledge must influence the bed inference, for radio-echo sounding can only impose some constraints on the bed topography, not determine it exactly. For example, the envelope itself is consistent with all the data; however, on those grounds, the locus-intersection cusps would not be interpreted as bed features. A dense array of loci, from a continuum of observation points along the flight path, would eliminate these cusps, but it would still yield only an upper-bound constraint on the actual bed topography.

The locus (eqs. 5) may be differentiated to give its slope, a convenient expression for which is

$$\frac{dz}{dx}=\tan\phi=\sin\theta\,(n^2-\sin^2\theta)^{-1/2}\ . \qquad (6)$$

The maximum value $dz/dx=0.679$ occurs at the maximum value $\phi=34.18°$. A second differentiation yields

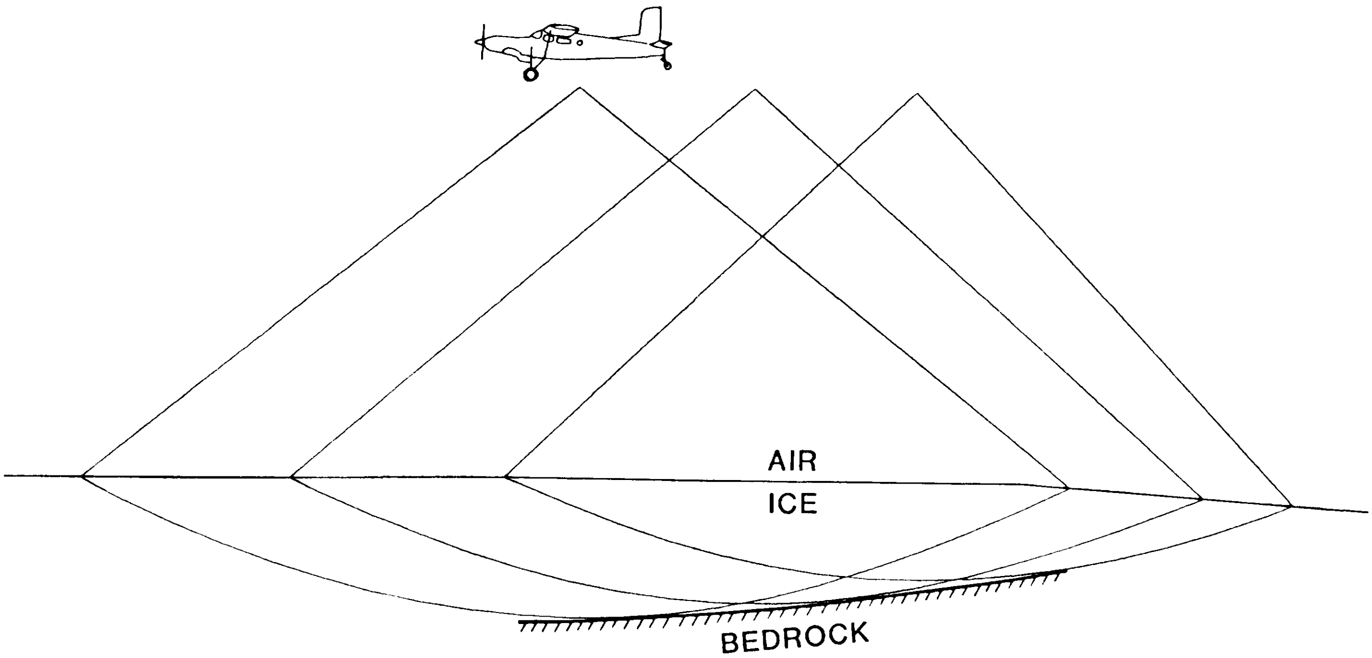

FIGURE 11.—Reflection loci from several positions along a flight path. A bed profile that is consistent with these hypothetical loci, but that is not uniquely determined by them, is also shown.

the radius of curvature, which may be written in the form

$$R = \left[1+\left(\frac{dz}{dx}\right)^2\right] \left\{nH\left[1-(n^2-1)\left(\frac{dz}{dx}\right)^2\right]^{-3/2} - z\right\} . \quad (7)$$

At $x=0$, where $dz/dx=0$, the radius is $R=nH-z$. This is significant because the radius increases at the same rate as the depth increases, but it increases n times faster than the airplane altitude increases. For a surface sounding ($H=0$), the radius of curvature at $x=0$ equals the depth. The ratio of these two, $R(0,z)/R(H,z)$, as a function of the ratio of the airplane altitude to the depth, is shown in figure 12. The radius of curvature may also be considered a function of the slope at some particular depth. The ratio $R(H,z,0)/R(H,z,|dz/dx|)$ as a function of the slope is shown in figure 13 for selected values of the ratio of the airplane altitude to the depth. These two diagrams demonstrate that as airplane altitude increases, the radius of curvature of the locus increases very rapidly—and so does the smallest scale of bed features that can be inferred from the data.

Errors in the calculation of the bed altitude can be related to errors in the original data. It is easily seen from equations 5 that at $x=0$ and error of $\delta z=8.43$ m

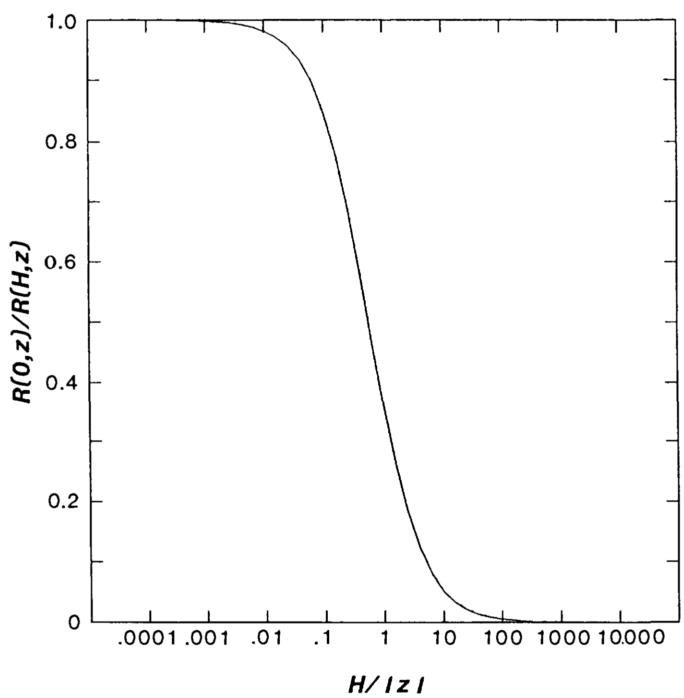

FIGURE 12.—Effect of airplane altitude on the radius of curvature of the reflection locus. For both the surface sounding and the sounding from airplane altitude H, the radius of curvature R is for the nadir, at depth z, where the slope of the locus is $dz/dx=0$ (eq. 7). A horizontal glacier surface is assumed.

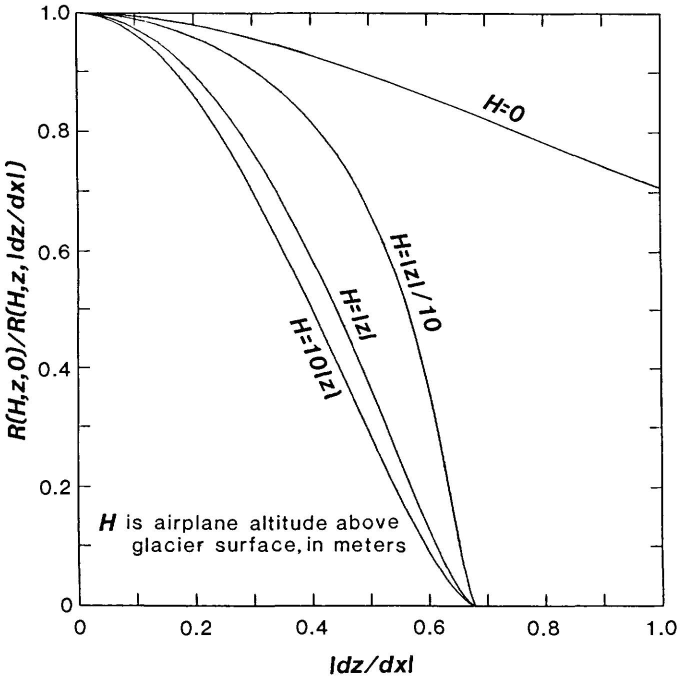

FIGURE 13.—Effect of the locus slope on the radius of curvature of the reflection locus (R). Two reflection loci at depth z are both from airplane altitude H but from different airplane positions, so that one has locus slope dz/dx and the other has zero slope. The radius-of-curvature ratio is given as a function of slope for selected H-to-$|z|$ ratios, including the special $H=0$ case of surface soundings (eq. 7). A horizontal glacier surface is assumed.

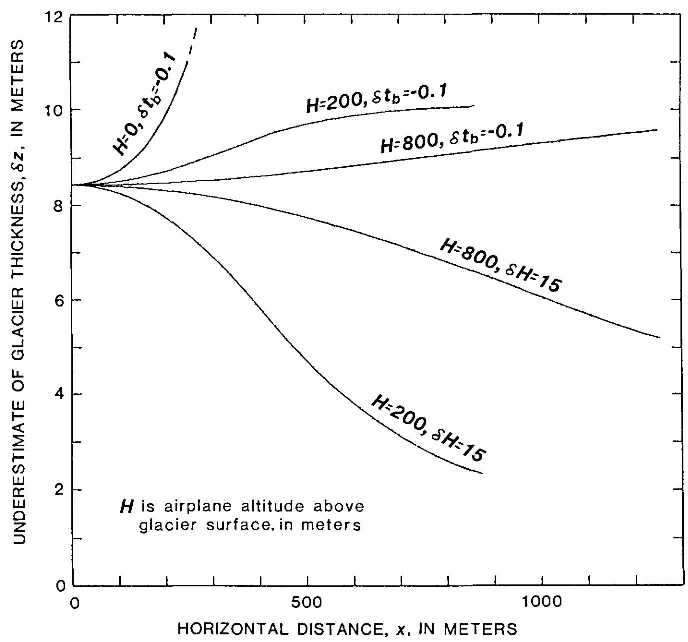

FIGURE 14.—Effects of errors in echo arrival time and airplane altitude. For the three reflection loci shown in figure 10, the underestimate δz of the glacier thickness is shown as a function of horizontal distance, for errors in arrival time $\delta t_b=-0.1$ microseconds and in airplane altitude $\delta H=+15$ meters. Only part of the $H=0$ curve is shown; this error increases very rapidly, because the locus from a surface sounding becomes so steep as the locus approaches the glacier surface (fig. 10).

may be produced by an error of either $\delta t_b=-0.1$ μs or of $\delta H=15$ m, regardless of the depth z. Elsewhere it is more complicated, as δt_b produces a greater change than the comparable δH does; the influence of δH is subdued by a cos θ-effect, whereas δt_b acts directly along the ray path. The sensitivity of the loci of figure 10 to errors of $\delta t_b=-0.1$ μs and $\delta H=15$ m is illustrated in figure 14. Whereas a small δt_b for a surface sounding produces a large δz at a large horizontal distance, the envelope of a profile of surface soundings (fig. 11) would be no more affected by that δt_b than a profile of aerial soundings.

Inferring the bed topography from radio-echo sounding data is an inverse problem, many characteristics of which are readily revealed by considering the forward problem. A hypothetical bed topography, having no variation in the other horizontal direction and underlying a horizontal glacier surface, is shown in figure 15. It also shows the envelope that would be obtained from loci constructed from arrival times that would be received from that bed along flight paths at $H=200$ and 800 m above the glacier surface and at the surface itself. A slight idealization is invoked at each end of the bed profile (points A and M), where it is assumed that a high curvature feature exists having the capability of reflecting back along the path from which it came a ray that might have come from any direction; otherwise, an echo would not be received at sounding positions near that same end, for the ray could not be normal to the bed at its endpoints. Were this not assumed, no echoes would be received toward the ends of the sounding profiles.

As would be expected from equation 7, the greater the altitude from which the sounding is done, the less detail is obtained in the envelope and the greater the error is. In fact, the 800-m profile is controlled by just short stretches of each of the five bed prominences (A, C, E, G, M); they control only part of the 200-m profile, which also receives echoes from bed points between the five prominences, and they control even less of the profile of soundings taken from the glacier surface. The range of control of each of these five stretches is indicated by the refracted ray making up the beginning and the end of each range.

The bed profile in figure 15 was composed so as to emphasize several different effects (eq. 7) on the curva-

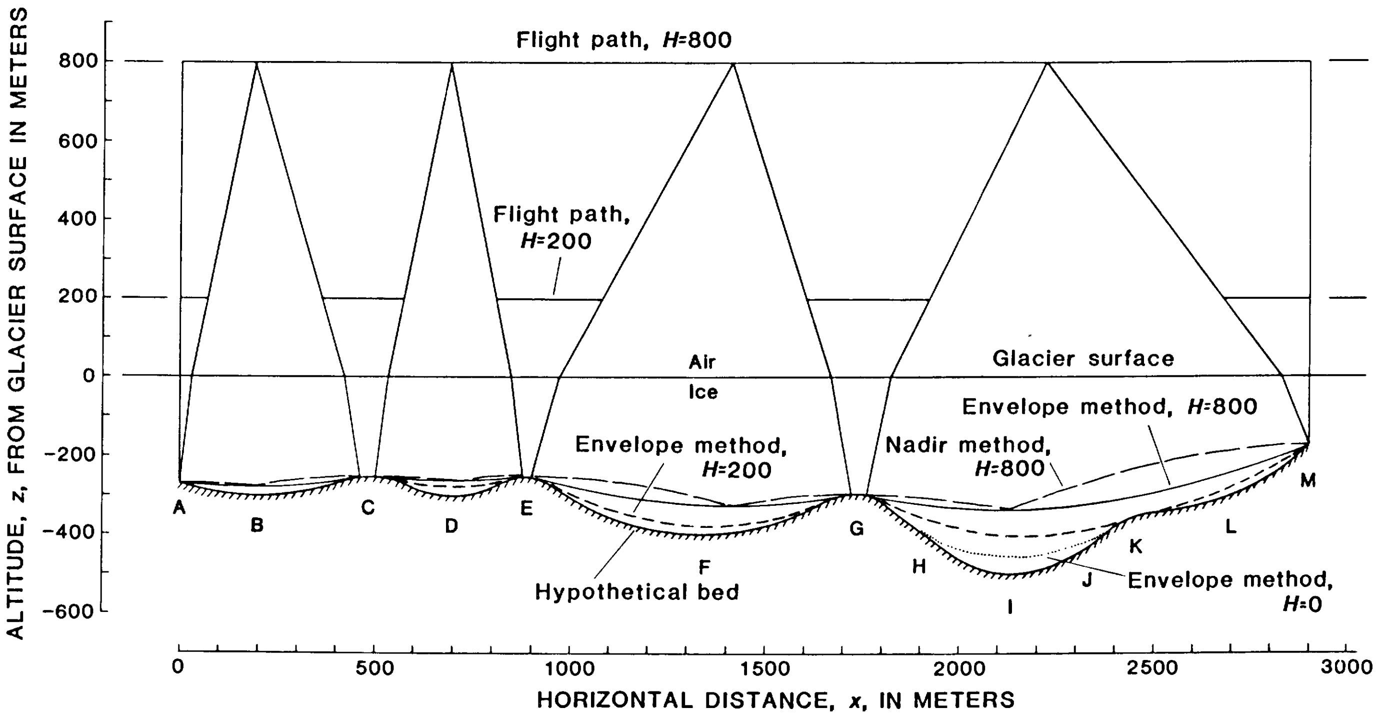

FIGURE 15.—Hypothetical bed profile and profiles inferred from echoes received at different altitudes. Over those segments where an inferred profile is not indicated, it is understood to be coincident with the bed. The ranges of control of each of the five prominences, which collectively control the entire record of soundings from 800 meters, are indicated by the refracted rays making up the beginning and end of each range. The discussion in the text is keyed to the lettered features.

ture of the reflection locus. Because of the effect of airplane altitude, the depression at B is detected in the 200-m data but not in the 800-m data. Because of the effect of depth below the surface, the depression at B is detected in the 200-m data but the one at F, which has the same curvature, is not; the same is true of the depressions at D and I with respect to the data from soundings at the surface. The depression at D—which is at the same depth as the one at B but has greater curvature—is not detected in the 200-m data, whereas the one at B is. The depression at L has the same depth and the same curvature as the one at B, but it is inclined from the horizontal; thus, the one at B is detected in the 200-m data but the one at L is not.

A separate effect occurs at H, J, and M, where the bed slope exceeds the maximum value of 0.679 that a locus from an aerial sounding can achieve. Therefore, these steep stretches could not be detected by any aerial data. The separation of the surface-sounding envelope from the bed at H and J is not caused by the steepness of the bed slope, but rather by the curvature of the depression at I.

Shown also in figure 15 is the bed profile that would be obtained from the 800-m data were the echo assumed to come always from the nadir. If the apropriate linear transformation ($ct=800n-z$) is made to the vertical scale, then the 800-m nadir curve becomes the $t_b(x)$ curve of the original data. The curves arising from making the same assumption with the 200-m and surface data are omitted for reasons of graphical clarity, but all six different bed inferences are briefly summarized in table 1.

Persistently reflecting points on the glacier bed generate hyperbolic segments (Harrison, 1970) on the signal profile $t_b(x)$, whether soundings are taken from the glacier surface or from above it. Such a hyperbolic segment is the nadir-method curve from $x=2{,}140$ to 2,900 m of figure 15, which is the same as the $t_b(x)$ profile if the appropriate linear transformation is made to the vertical scale. Five such hyperbolas are shown in figure 16 for persistently reflecting points at depths of 200 and 500 m as detected from the glacier surface and from altitudes of 200 and 800 m above it. The slope dt_b/dx is zero at $x=0$, where the sounding is taken from directly above the reflecting point. It may be shown that the limiting slope, at $x=\infty$, is $dt_b/dx=2/c=6.7$ μs/km for surface soundings, and is $dt_b/dx=2n/c=11.9$ μs/km for soundings taken from above the surface.

TABLE 1.—*Summary of errors in inferring bed profile of figure 15, using each of the two methods, on data from each of three indicated altitudes*
[m, meters]

	Envelope method			Nadir method		
	H=0	H=200 m	H=800 m	H=0	H=200 m	H=800 m
Root-mean-square error --- (m)	13	33	67	34	57	90
Maximum error --------- (m)	44	96	163	90	129	186
Location, x --------------- (m)	2,140	2,120	2,150	2,000	2,050	2,240

REFRACTION AND REFLECTION REPRESENTED IN THREE DIMENSIONS

The two-dimensional representation of the refraction-reflection geometry is easily extended to three dimensions. For the case of a horizontal glacier surface, the complete locus is the body of revolution formed by rotating the x,z locus (fig. 10) about the z-axis. If the surface is not horizontal, but is planar, the rotation is about the normal to the plane.

Snell's law (eq. 3) is easily expressed in three dimensions. The point (x_1,y_1,z_1) on the air ray and the point (x_2,y_2,z_2) on the ice ray are each a unit distance from the origin, which is where the refraction occurs (fig. 17).

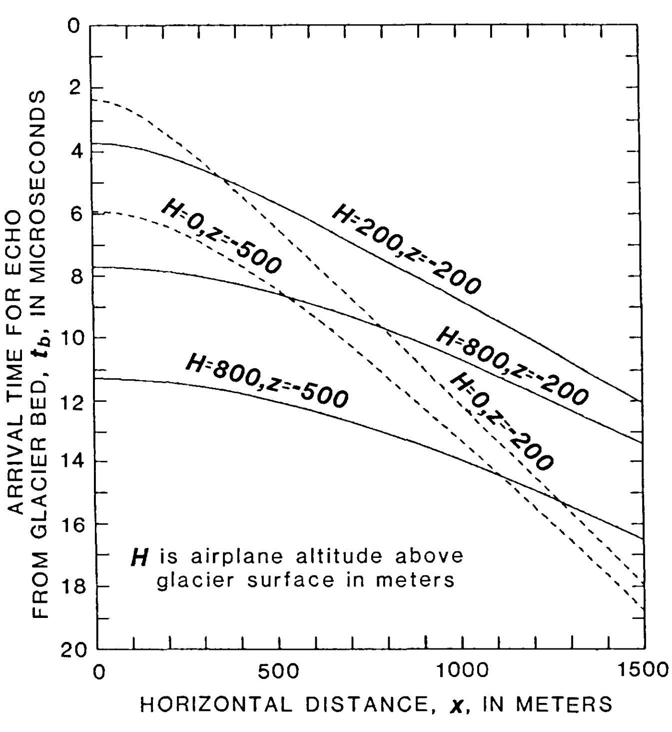

FIGURE 16.—Arrival-time hyperbolas caused by hypothetical persistently reflecting points on the glacier bed. Each $t_b(x)$ hyperbola is identified by the depth z of the point below the horizontal glacier surface and by the altitude H above it from which the point is detected. The horizontal distance from the point is x.

The plane $\alpha x+\beta y+\gamma z=0$ has its coefficients scaled as to magnitude and sign so that, respectively, $\alpha^2+\beta^2+\gamma^2=1$ and $\alpha x_1+\beta y_1+\gamma z_1=\cos\theta>0$. Then,

$$\begin{pmatrix} x_1 \\ y_1 \\ z_1 \end{pmatrix} + n \begin{pmatrix} x_2 \\ y_2 \\ z_2 \end{pmatrix} = k \begin{pmatrix} \alpha \\ \beta \\ \gamma \end{pmatrix}, \qquad (8)$$

in which

$$k=\cos\theta-(n^2-\sin^2\theta)^{1/2}=(1-n^2\sin^2\phi)^{1/2}-n\cos\phi$$

and

$$-\cos\phi=\alpha x_2+\beta y_2+\gamma z_2 .$$

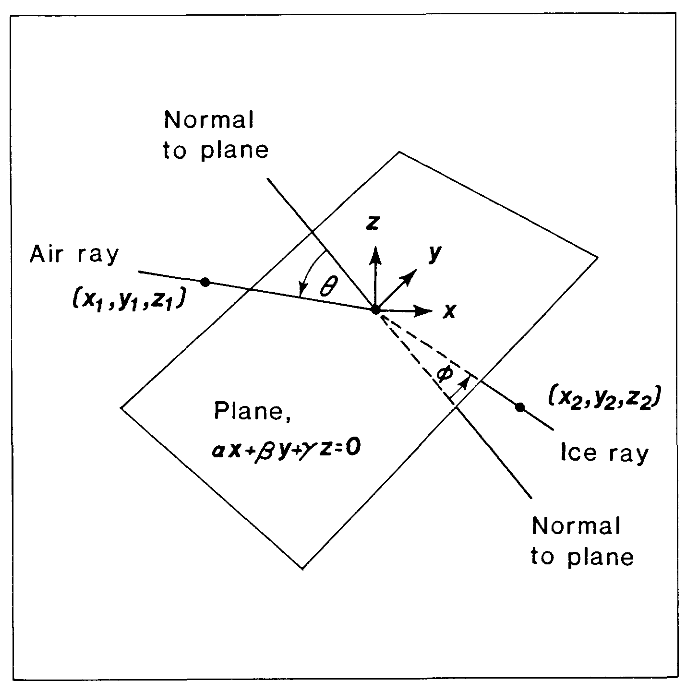

FIGURE 17.—Snell's law in three dimensions. The angles θ and ϕ obey equation 3. The points (x_1,y_1,z_1) and (x_2,y_2,z_2), each a unit distance from the refraction point, are related by equation 8.

Either the θ-form or the ϕ-form of k is used, according to whether (x_2,y_2,z_2) is found from (x_1,y_1,z_1) or the other way around. The plane determined by the two rays is normal to the refracting plane. The signal's travel time between (x_1,y_1,z_1) and (x_2,y_2,z_2) is less when passing through the origin than it would be were it to pass through any other point in the plane. In the analysis of the Columbia Glacier data, a plane was used to approximate the surface topography lying between an airplane position and a location where the altitude of the reflection locus is desired.

If the glacier bed is idealized as a differentiable, mathematical surface, then a normal exists at every point on the bed. A ray that strikes the bed at some point by following some path other than along the normal will be reflected, but it will not return along the same path. Because the airplane's motion is negligible compared with the speed at which the signal travels, only a ray that travels along a normal to the bed will produce an echo that reaches the airplane. Equivalently, an echo will be received only from points where the three-dimensional reflection locus is tangent to the bed. For any particular point on the bed, then, an echo can be received at only one particular airplane position at any particular altitude. Because the ray path must be normal to the bed, its direction cosines are uniquely determined by the direction cosines of the bed at that point. This unique ray path through the ice is refracted at the glacier surface, according to Snell's law, into a unique ray path through the air.

It is also assumed that the laws of geometric optics apply; that is, the wavelength of the signal is much smaller than the roughness elements on the bed. Small-scale roughness, which could not be analyzed, could cause an unknown amount of diffraction or other effects that might complicate the analysis.

COLUMBIA GLACIER DATA

The echo arrival times t_b for the 678 airplane positions (fig. 4) are tabulated in appendix A. The arrival times for the airplane-bed-airplane round trip are in microseconds. A frequency distribution of the altitude H of the airplane above the glacier surface appears as figure 6. Arrival times were read at about every 5 mm along the reconstructed profile; if the maximum value of t_b for the east-west flight paths did not occur at one of these equally spaced positions, an extra point at the maximum t_b location was also included because it gives the greatest depth to the bed.

The reflection lobes implied by the set of coordinates (x, y, z, t_b) for each of the 678 airplane positions were constructed by using a plane to approximate the glacier surface locally. At each node of a 200-m square grid, the altitudes of all lobes reaching that node were compared, and the deepest one was taken to be the envelope altitude there. The bed topography was inferred by contouring the unadjusted envelope altitudes (fig. 18) except near the terminus, where directly measured bathymetry was used.

A vertical cross section (fig. 19) shows the relationship between the reflection lobes and their envelope for one flight path. The section, along $y=15.4$ km, was chosen because the contours are nearly north-south in direction, so that there is little transverse bed slope. It demonstrates that the normality condition is satisfied in the x,z plane, because where the refracted rays reach the envelope they are normal to it. An indication that the normality condition is satisfied in the x,y plane is provided by figure 20, which shows at each grid node which one of the reflection lobes forms the envelope there; the straight line joining the center of the reflection lobe and the node is generally normal to the contour there. The fact that the envelope is reached by almost all of the reflection lobes is evidence of the high internal consistency of the data.

The envelope near the terminus is made up of lobes from airplane positions that are about a kilometer upglacier (figs. 4, 20). Because the echoes having the arrival times that determine these lobes are likely from bed locations near the flight path, the envelope near the terminus is artificially shallow. This is confirmed by the direct bathymetric measurements, some of which were made since the terminus retreated behind its August 26, 1978, position (Post, 1975; Post, written commun., 1979–1984). The inferred bed topography (fig. 18) is taken to be the directly measured bathymetry—where it exists—and in a slender zone upglacier from there it is taken to be an interpolation between it and the envelope of the reflection lobes. The adjustment made to the envelope (fig. 21) is greatest near the terminus, where the directly measured bathymetry exists and where the airborne coverage is poor, and fades to zero at the upglacier margin of the interpolation zone.

The difference between the nadir method and the envelope method is shown in figure 22, which also shows the difference between the envelope method and the reflection lobes from some surface soundings. Where the envelope directly beneath an airplane position is horizontal, the nadir method and the envelope method give the same result; if the bed has any inclination, the nadir method gives a shallower estimate of the bed altitude. Whereas the envelope-method bed is contoured from values on the 200-m square grid, the difference between the nadir method and the envelope method exists only directly beneath an airplane position; therefore, the contouring of the difference is less

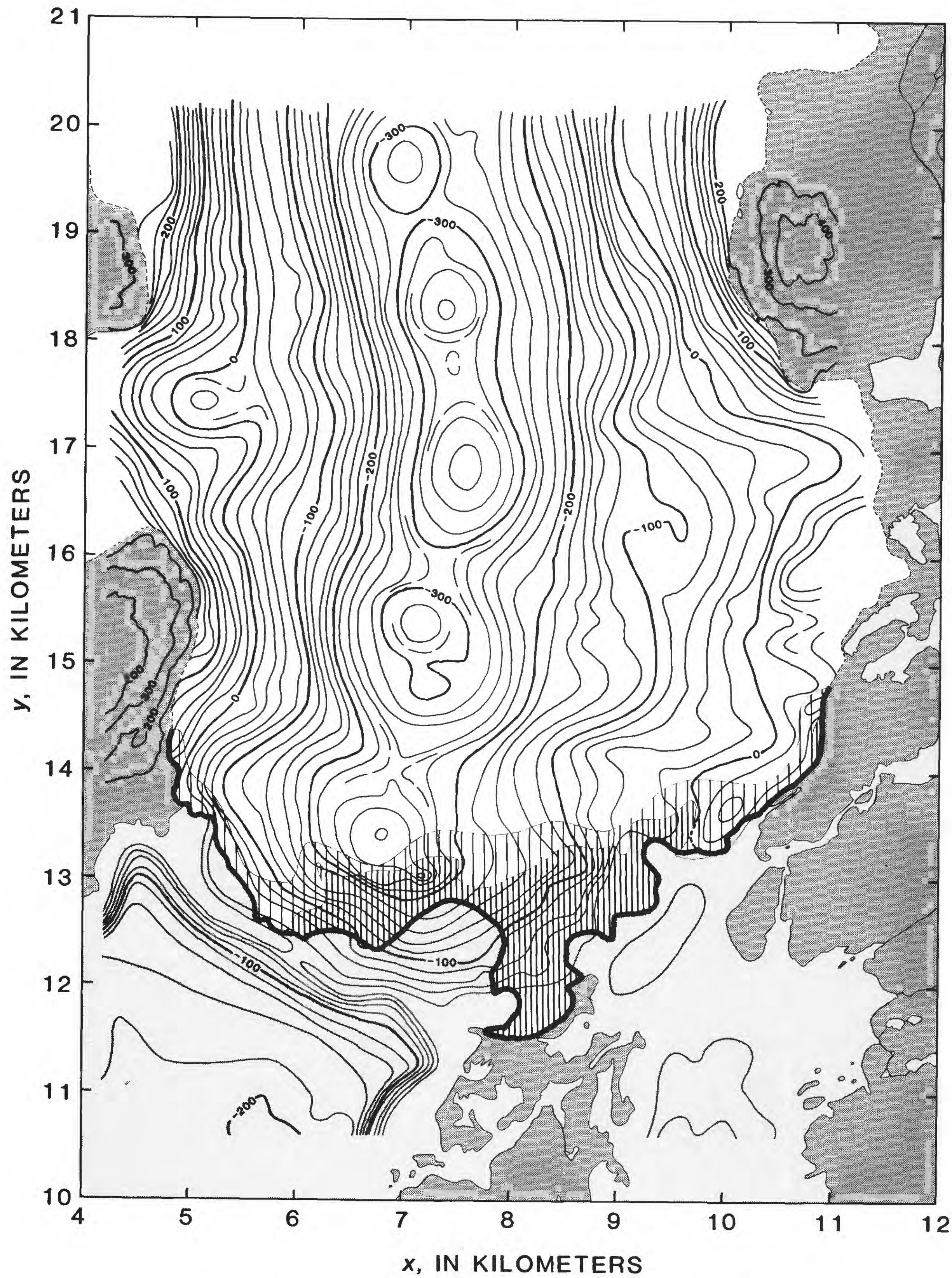

y, IN KILOMETERS
x, IN KILOMETERS
-300
-200
-100
0
100
200
300
400

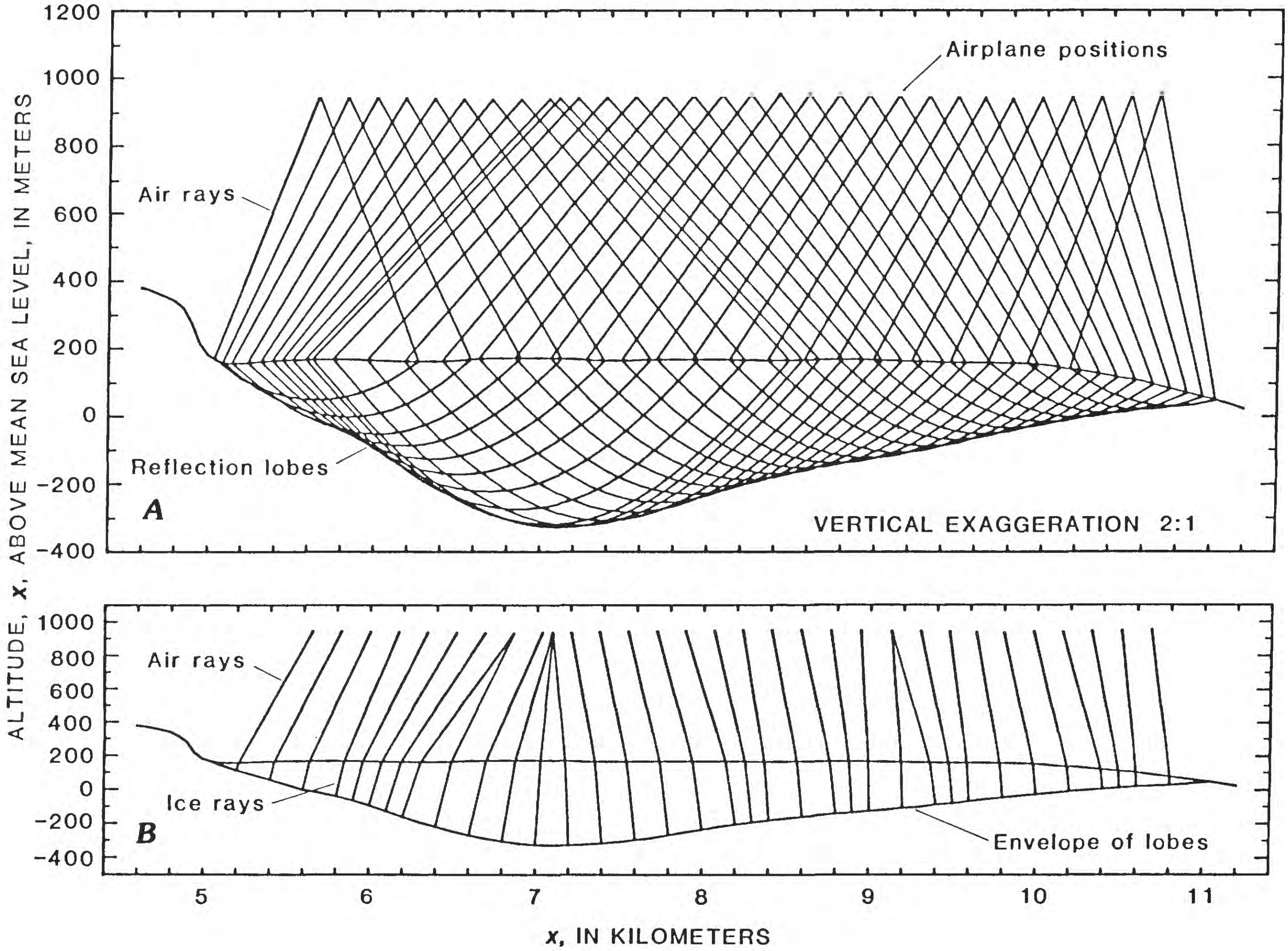

FIGURE 19.—Vertical cross section along $y = 15.4$ kilometer showing glacier surface and reflection lobes for 31 positions along flight path N2500. For each airplane position are shown (A) the vertical cross section through its reflection lobe as well as the air rays from the intersections of the lobe and the glacier surface, and (B) the air ray refracted at the glacier surface into the ice ray that reaches envelope of lobes. In (B) are shown the envelope and those rays reaching it at integral multiples of 200 meters along the x-axis; also shown are some rays at intermediate points on the envelope from airplane positions for which the lobe does not form the envelope at any 200-meter multiple. For clarity, the lobes from other flight paths are not shown; the actual envelope is slightly deeper, by as much as 5 meters at $x = 5.8$, 6.4, and 7.8 kilometers.

FIGURE 18.—Inferred bed topography. Contour interval is 100 meters on exposed bedrock and 20 meters elsewhere. Terminus position (heavy solid curve) is taken from August 26, 1978, vertical aerial photography. Bed topography in front of terminus and in densely ruled region behind terminus is taken from direct bathymetric soundings (Austin Post, written commun., 1979–1984). Bed topography in sparsely ruled region is taken from an extrapolation of the adjustment (fig. 21) in the densely ruled region.

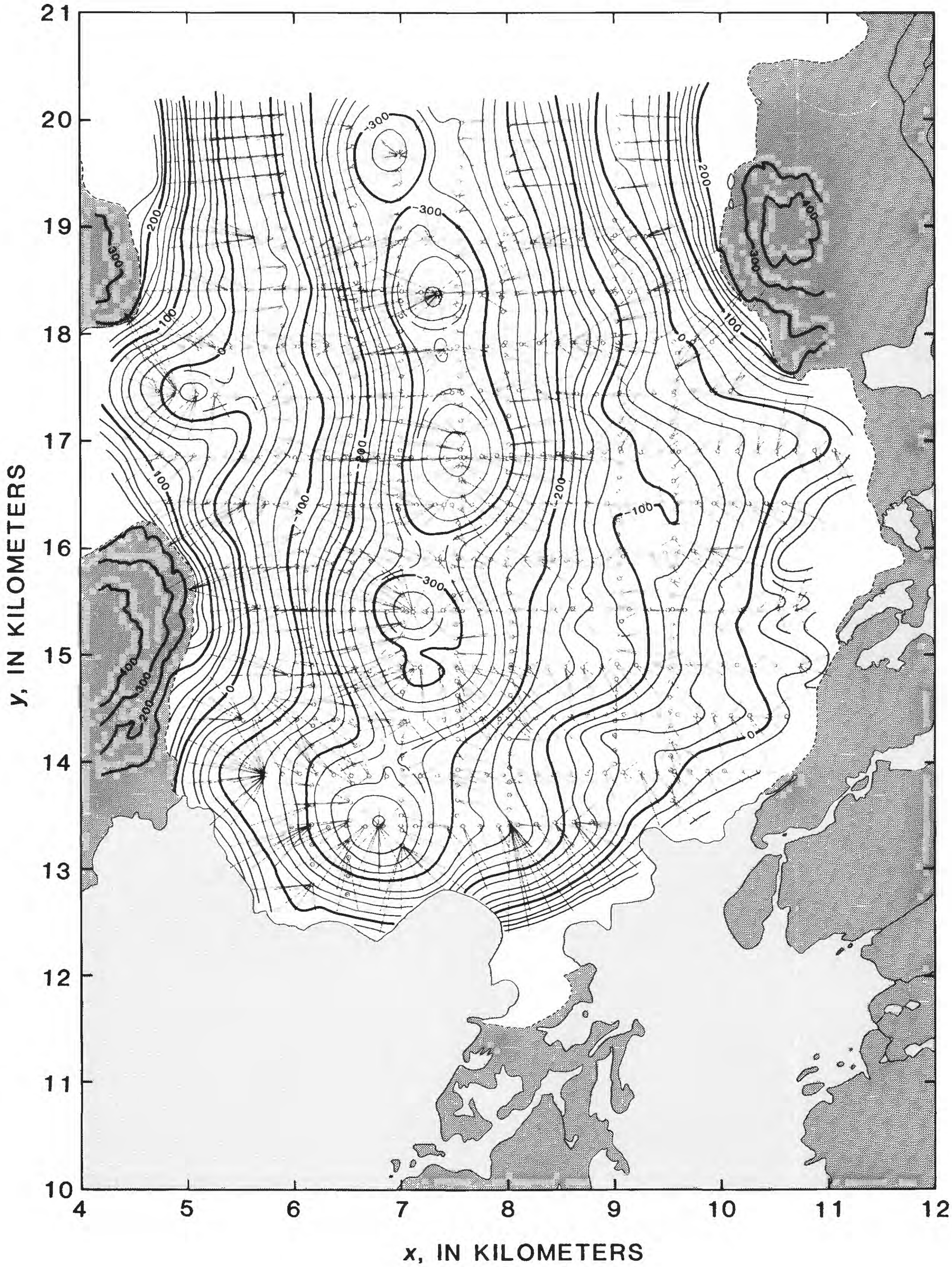
21
20
19
18
17
16
15
14
13
12
11
10
4
5
6
7
8
9
10
11
12
y, IN KILOMETERS
x, IN KILOMETERS
-300
-200
-100
0
100
200
300
400

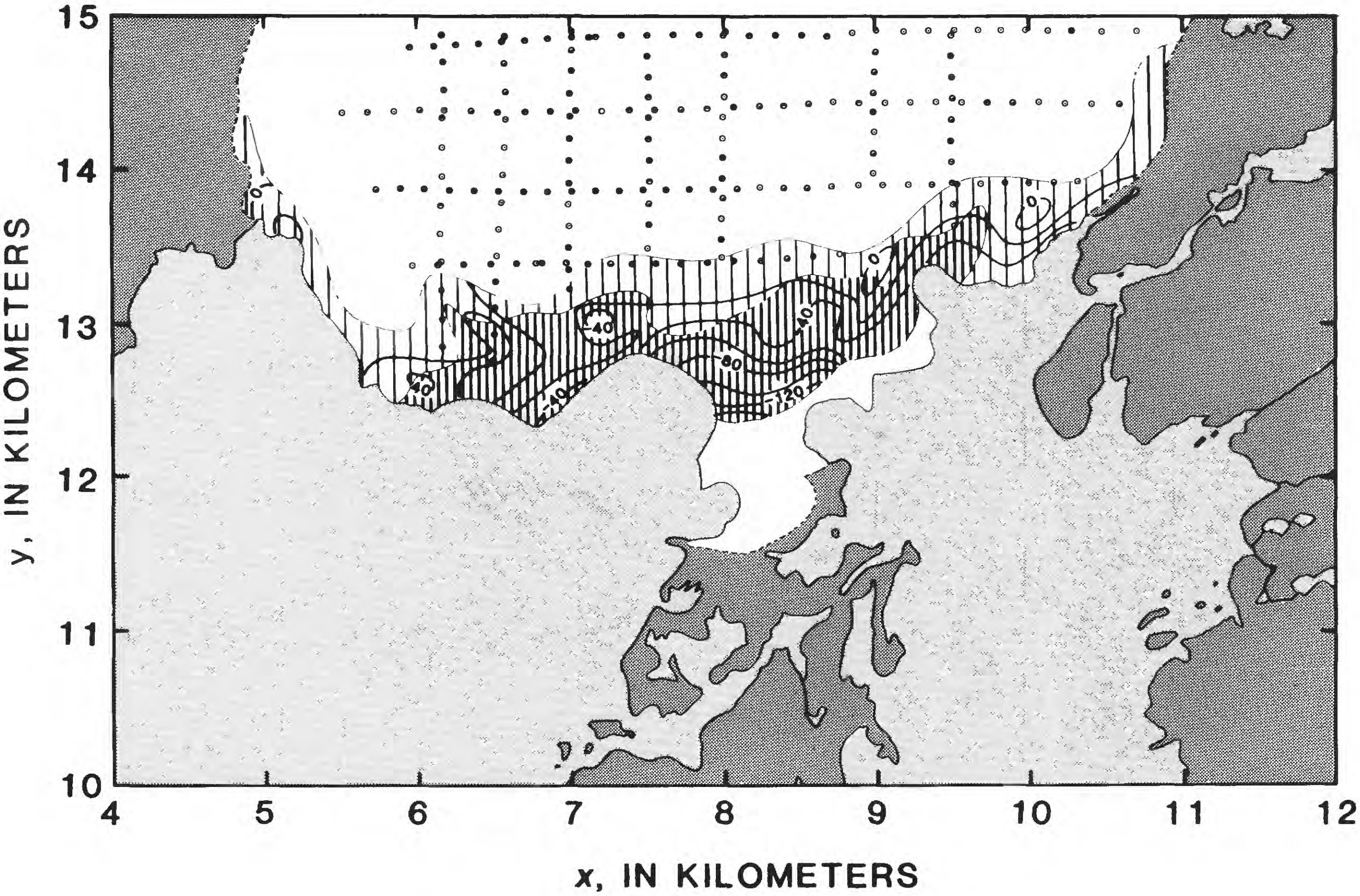

FIGURE 21.—Adjustment of envelope-method bed according to directly measured bathymetry (Austin Post, written commun., 1979–1984), a negative value indicating lowering of the inferred altitude. Contour interval is 20 meters. The adjustment in the sparsely ruled region is an extrapolation of the adjustment in the densely ruled region, where direct bathymetry was taken. The amount of the adjustment is not defined all the way down to the August 26, 1978, terminus position because the envelope method could not be applied that far away from the airplane positions (dots) from which echo arrival times are available.

FIGURE 20.—Sources of reflection lobes forming envelope of lobes. For each node of the 200-meter square grid is shown the airplane position (small circle) whose reflection lobe forms the envelope at that node. At some intermediate points are shown the airplane position whose lobe forms the envelope at that point but does not form the envelope at any grid node. For a few airplane positions, the echo arrival time presumably was underestimated, so that the resulting lobe was too shallow to reach the envelope. The bed contours shown are those obtained from the envelope method without modification according to the directly measured bathymetry.

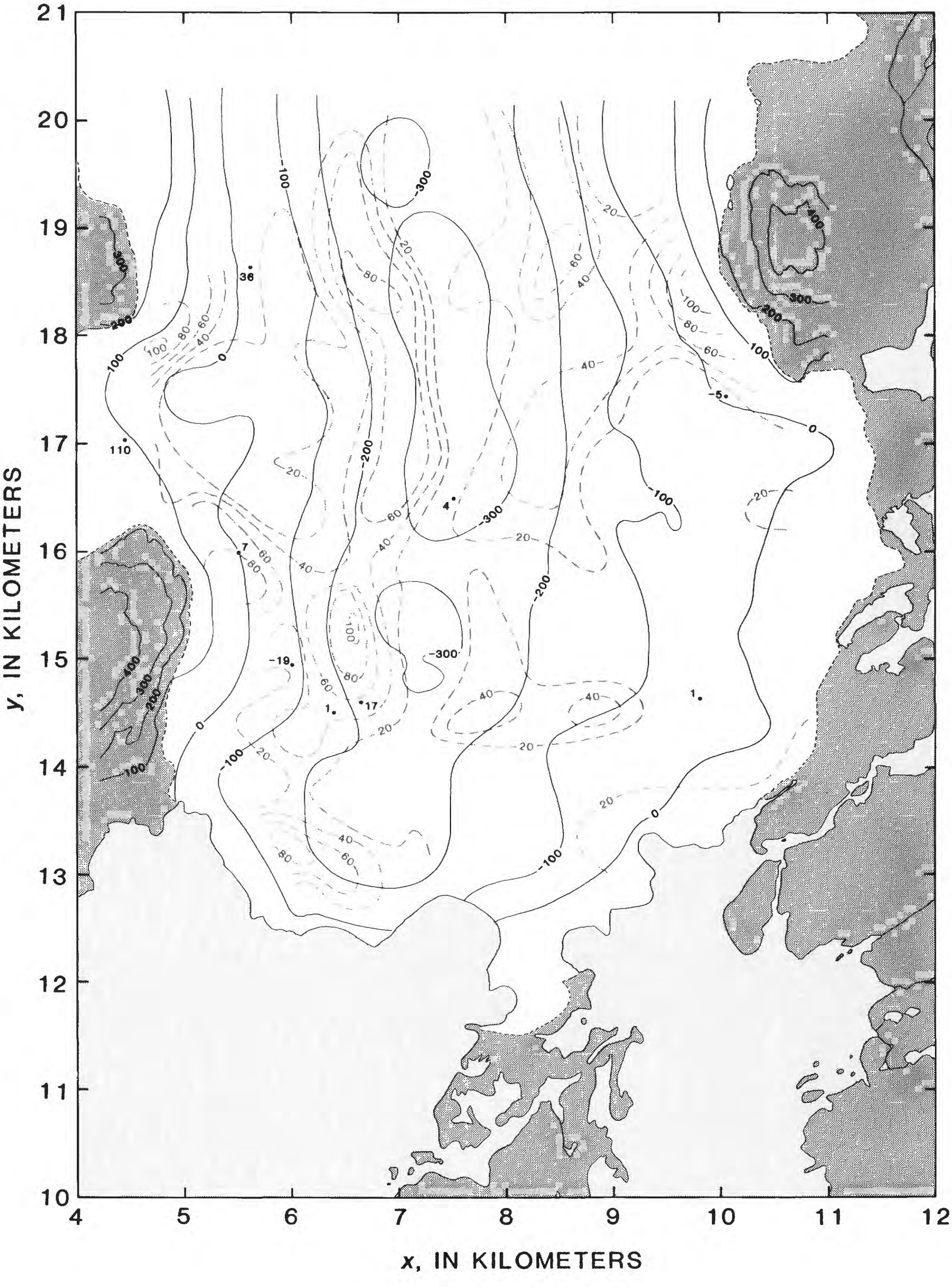
y, IN KILOMETERS
x, IN KILOMETERS

accurate than the contouring of the envelope-method bed. The maximum difference between the envelope-method bed and a surface sounding, however, does not occur directly beneath the position from which the sounding was taken unless the envelope-method bed is horizontal there. The location and the amount of the algebraically maximum height of the envelope-method bed above the sphere, which is the reflection lobe of the surface sounding, are shown in figure 22.

DISCUSSION

If there is a strong law that says that every echo must come from someplace and that the bed there must be normal to the refracted ray, then there is probably also a weak law that says that an echo comes from only one place. Were the weak law valid, then the regions where it is likely that the bed altitude is overestimated are those regions where the envelope at many grid nodes is formed by a single reflection lobe; according to this weak law, the bed coincides with the envelope at only one point within such a region and is below it elsewhere. Several candidates for such regions are revealed by the source map (fig. 20). The most conspicuous occurrence of this is the sequence of closed depressions along the bottom of the valley, where the curvature of the bed likely exceeds that of the reflection lobes. Each of the dominating lobes here is produced by the maximum t_b of an east-west profile. Were the data free of error, the true bed altitude would be given at one point per reflection lobe and the altitude of the bed would be overestimated elsewhere. The resulting surface will be much smoother than the actual bed topography. When the airplane is 800 m above ice that is 500 m thick, and the bed slope does not exceed 0.2, the radius of curvature of the reflection lobe is about 2,000 m (eq. 7; figs. 12, 13).

In addition, data error must be considered. For one thing, it may be the reason some reflection lobes apparently do not reach the envelope (fig. 20). It would be possible to adjust the t_b to make such a lobe reach the envelope—which is the ultimate test of internal consistency of the data—but this would not modify the envelope, which is what the bed topography is inferred from. The effect of errors in t_b or H can be determined from equations 5, as illustrated in figure 14. The estimated 0.36 μs error in t_b, assuming the airplane altitude to be exactly 800 m, corresponds to an error of about 30 m for the point on the lobe directly beneath the airplane, and an error of about 35 m at a horizontal distance of 1 km. Conversely, if t_b is correct, the estimated 30-m error in airplane altitude corresponds to an error of about 17 m directly beneath and about 12 m one kilometer away.

A biased error distribution in the inferred bed topography results. Bed prominences control the data and cause overestimation of the bed altitude elsewhere, whereas the data error may induce an error of either sign.

This project was not only the first airborne radio-echo sounding of a temperate glacier, but it also was performed under a severe time constraint. If time had allowed testing of the entire system—including the data analysis—prior to the actual sounding of Columbia Glacier, many of the problems encountered would have been recognized and solved. With this in mind, there are a few fundamental suggestions to those interested in work on airborne radio-echo sounding of temperate glaciers.

First, in order to infer a glacier bed topography from airborne radio-echo sounding, it is necessary to have the location of the initial pulse (the flightline on the reconstructed photograph), t_b, and knowledge of the glacier surface topography. The last can be obtained by recording t_s, by having a known surface topography, or by recording both the barometric and radar altitudes. Because of the possible error due to changing atmospheric conditions, the barometric altimeter needs to be carefully calibrated before and after each flight.

Second, when attempting to sound a deep, narrow, temperate, valley glacier, the gross geometry of the wave—the radius of curvature of the reflection lobe increases at the rate of 1.78 times H—necessitates flying as close to the glacier surface as possible. Thus, the dead time of the system (a minimum of 3.5 μs in this case) must be reduced.

Finally, careful consideration needs to be given to the data acquisition system and to the data reduction. It is necessary to think through completely what data are desired and how they will be analyzed, so it can be

FIGURE 22.—Nadir-method results and surface soundings. Solid contours (100-meter interval) show exposed bedrock and bed topography inferred by the envelope method; they agree with figure 18 except in its ruled regions, where they differ by the amount shown in figure 21. Dashed contours (20-meter interval) show height of nadir-method bed above envelope-method bed. Spot values show the difference, in meters, between the envelope-method bed and surface soundings (Mayo and others, 1979), a positive value indicating that the envelope method gave a higher altitude.

determined what variables should be measured and in what format the measurements should be recorded. The system should also allow easy recovery of the raw recorded data.

REFERENCES CITED

Bindschadler, R.A., and Rasmussen, L.A., 1983, Finite-difference model predictions of the drastic retreat of Columbia Glacier, Alaska: U.S. Geological Survey Professional Paper 1258–D, 17 p.

Bishop, J.F., Cumming, A.D.G., Ferrari, R.L., Miller, K.J., and Owen, G., 1979, The 1977 Cambridge University expedition to Vatnajökull, Iceland: Cambridge, University of Cambridge, Dept. of Engineering, Special Report 6.

Björnsson, Helgi, 1982, Drainage basins on Vatnajökull mapped by radio echo soundings: Nordic Hydrology, v. 13, no. 4, p. 213–232.

Björnsson, Helgi, Ferrari, R.L., Miller, K.J., and Owen, G., 1977, A 1976 radio echo sounding expedition to the Vatnajökull Ice Cap, Iceland: The Polar Record, v. 18, no. 115, pp. 375–377.

Brown, C.S., Meier, M.F., and Post, Austin, 1982, Calving speed of Alaska tidewater glaciers, with application to Columbia Glacier: U.S. Geological Survey Professional Paper 1258–C, 13 p.

Churchill, R.J., and Wright, D.L., 1978, An airborne radio-echo sounder for measurements in temperate glaciers: Colorado State University Department of Electrical Engineering, Final Report, 63 p.

Evans, S., 1963a, Radio techniques for the measurement of ice thickness: The Polar Record, v. 11, no. 73, p. 406–410.

———1963b, International co-operative field experiments in glacier sounding: Greenland, 1963: The Polar Record, v. 11, no. 75, p. 725–726.

———1963c, Correspondence: Radio techniques for the measurement of ice thickness: The Polar Record, v. 11, no. 75, p. 795.

———1967, Progress report on radio echo sounding: The Polar Record, v. 13, no. 85, p. 413–420.

Ferrari, R.L., Miller, K.J., and Owen, G., 1976, The 1976 Cambridge-Reykjavik Universities expedition to Vatnajökull, Iceland: Cambridge, University of Cambridge, Dept. of Engineering, Special Report 5, 62 pp.

Fountain, A.G., 1982, Columbia Glacier photogrammetric altitude and velocity: Data set (1957–1981): U.S. Geological Survey Open-File Report 82–756, 226 p.

Harrison, C.H., 1970, Reconstruction of subglacial relief from radio echo sounding records: Geophysics, v. 35, no. 6, p. 1099–1115.

Kollmeyer, R.C., Motherway, D.L., Robe, R.Q., Platz, B.W., and Shah, A.M., 1977, A design feasibility study for the containment of icebergs within the waters of Columbia Bay, Alaska: U.S. Coast Guard Final Report 128, 135 p.

Mayo, L.R., Trabant, D.C., March, Rod, and Haeberli, Wilfried, 1979, Columbia Glacier stake location, mass balance, glacier surface altitude, and ice radar data—1978 measurement year: U.S. Geological Survey Open-File Report 79–1168, 72 p.

Meier, M.F., Post, Austin, Brown, C.S., Frank, David, Hodge, S.M., Mayo, L.R., Rasmussen, L.A., Senear, E.A., Sikonia, W.G., Trabant, D.C., and Watts, R.D., 1978, Columbia Glacier progress report—December 1977: U.S. Geological Survey Open-File Report 78–264, 56 p.

Meier, M.F., Rasmussen, L.A., Post, Austin, Brown, C.S., Sikonia, W.G., Bindschadler, R.A., Mayo, L.R., and Trabant, D.C., 1980, Predicted timing of the disintegration of the lower reach of Columbia Glacier, Alaska: U.S. Geological Survey Open-File Report 80–582, 47 p.

Meier, M.F., Rasmussen, L.A., Krimmel, R.M., Olsen, R.W., and Frank, David, 1985, Photogrammetric determination of surface altitude, terminus position, and ice velocity of Columbia Glacier, Alaska: U.S. Geological Survey Professional Paper 1258–F, 41 p.

Morgan, V.I., and Budd, W.F., 1975, Radio-echo sounding of the Lambert Glacier Basin: Journal of Glaciology, v. 15, no. 73, p. 103–111.

Oswald, G.K.A., 1975, Investigations of sub-ice bedrock characteristics by radio-echo sounding: Journal of Glaciology, v. 15, no. 73, p. 75–87.

Post, Austin, 1975, Preliminary hydrography and historic terminal changes of Columbia Glacier, Alaska: U.S. Geological Survey Hydrologic Investigations Atlas 559, 3 sheets.

Rasmussen, L.A., 1985, Adjusting two-dimensional velocity data to obey continuity: Journal of Glaciology, v. 31, no. 108, p. 115–119.

Rasmussen, L.A., and Meier, M.F., 1982, Continuity equation model of the predicted drastic retreat of Columbia Glacier, Alaska: U.S. Geological Survey Professional Paper 1258–A, 23 p.

———1985, Surface topography of the lower part of Columbia Glacier, Alaska, 1974–1981: U.S. Geological Survey Professional Paper 1258–E, 63 p.

Robin, G. de Q., 1975, Radio-echo sounding: Glaciological interpretations and applications: Journal of Glaciology, v. 15, no. 73, p. 49–64.

Robin, G. de Q., Swithinbank, C.W.M., and Smith, B.M.E., 1970, Radio echo exploration of the Antarctic ice sheet: International Symposium on Antarctic Glaciological Exploration, Hanover, N.H., 1968, Proceedings, p. 97–115.

Sikonia, W.G., 1982, Finite-element glacier dynamics model applied to Columbia Glacier, Alaska: U.S. Geological Survey Professional Paper 1258–B, 74 p.

Sikonia, W.G., and Post, Austin, 1980, Columbia Glacier, Alaska: Recent ice loss and its relationship to seasonal terminal embayments, thinning, and glacier flow: U.S. Geological Survey Hydrologic Investigations Atlas 619, 3 sheets.

Smith, B.M.E., and Evans, S., 1972, Radio echo sounding: Absorption and scattering by water inclusion and ice lenses, Journal of Glaciology, v. 11, no. 61, p. 133–146.

Sverrison, Marteinn, Jóhannesson, Ævar, and Björnsson, Helgi, 1978, A radio-echo equipment for depth sounding of temperate glaciers: Reykjavik, Science Institute, University of Iceland, Report RH–78–16, 15 p.

Swithinbank, C.W.M., 1968, Radio echo sounding of Antarctic glaciers from light aircraft: IUGG/IASH General Assembly of Bern, 1967: Reports and discussions, p. 405–414.

Vancouver, George, 1798, A voyage of discovery to the North Pacific Ocean and round the world in the years 1790–1795: London, printed for G.G. and J. Robinson, Paternoster-Row, and J. Edwards, Pall-Mall, v. 3.

Vickers, R.S., and Bollen, Robert, 1974, An experiment in the radio echo sounding of temperate glaciers: Menlo Park, Calif., Stanford Research Institute, Final Report, 16 pp.

Watts, R.D., and England, A.W., 1976, Radio-echo sounding of temperate glaciers: Ice properties and sounder design criteria: Journal of Glaciology, v. 17, no. 75, p. 39–48.

Watts, R.D., and Wright, D.L., 1981, Systems for measuring thickness of temperate and polar ice from the ground or from the air: Journal of Glaciology, v. 27, no. 97, pp. 459–469.

APPENDIX A: ECHO ARRIVAL TIMES

The following tables give the echo arrival times at each airplane position along the 12 east-west and 7 north-south profiles. The numbers preceded by "N" or "W" indicate flight paths shown in figure 4. The arrival times (t) are the roundtrip airplane-bed-airplane signal times, in microseconds; x and y are the horizontal coordinates of the airplane in the local Columbia Glacier coordinate system (eq. 1), and z is the vertical coordinate, in meters above sea level.

x	y	z	t	x	y	z	t	x	y	z	t
N500				5967	13386	888	7.64	6137	13389	885	8.35
				6308	13392	882	8.83	6479	13395	880	9.22
6649	13398	877	9.55	6786	13400	876	9.80	6820	13401	874	9.70
6986	13403	874	9.38	7127	13398	884	9.17	7269	13394	895	9.04
7419	13389	906	8.92	7574	13387	914	8.80	7736	13395	917	8.68
7904	13403	919	8.54	8077	13411	921	8.38	8250	13419	924	8.18
8424	13428	926	7.93	8597	13436	928	7.62	8770	13444	930	7.20
N1000				5728	13874	996	8.82	5887	13884	1019	9.08
				6048	13881	1022	9.34	6210	13877	1022	9.60
6371	13873	1021	9.87	6533	13868	1020	10.13	6694	13864	1020	10.30
6854	13862	1020	10.33	7012	13865	1024	10.27	7169	13867	1028	10.16
7327	13870	1031	10.01	7484	13873	1035	9.83	7638	13875	1034	9.62
7791	13877	1032	9.40	7945	13879	1031	9.18	8098	13880	1029	8.97
8252	13882	1028	8.78	8405	13884	1026	8.60	8559	13886	1025	8.43
8719	13889	1022	8.26	8889	13896	1018	8.10	9057	13901	1017	7.95
9216	13903	1027	7.82	9374	13905	1038	7.69	9533	13907	1049	7.56
9692	13909	1060	7.44	9850	13911	1070	7.34	10009	13913	1081	7.24
10168	13915	1092	7.15	10326	13916	1103	7.06				
N1500				5509	14379	870	6.73	5678	14385	887	6.99
				5847	14391	905	7.28	6015	14397	923	7.60
6187	14395	924	7.94	6360	14388	914	8.30	6534	14381	904	8.67
6706	14380	900	9.05	6877	14384	901	9.41	7049	14387	902	9.77
7220	14391	903	9.59	7392	14395	904	9.34	7563	14398	905	9.14
7735	14402	905	8.91	7906	14405	906	8.66	8078	14409	907	8.40
8249	14412	908	8.15	8411	14423	911	7.92	8571	14435	914	7.71
8733	14443	917	7.53	8900	14441	915	7.41	9067	14439	913	7.38
9235	14437	911	7.37	9402	14435	910	7.35	9569	14433	908	7.31
9737	14431	906	7.22	9904	14429	905	7.07	10071	14427	903	6.88
10243	14425	907	6.65	10419	14424	918	6.38	10595	14422	928	6.08
N2000				5949	14809	1018	8.21	6101	14818	1022	8.40
				6252	14827	1026	8.72	6404	14836	1030	9.12
6555	14845	1034	9.57	6707	14854	1037	10.04	6858	14863	1041	10.53
7010	14872	1045	11.04	7126	14876	1044	11.40	7175	14878	1044	11.39
7339	14884	1043	11.34	7507	14885	1041	11.18	7675	14884	1038	10.81
7844	14883	1035	10.44	8012	14881	1032	10.11	8181	14880	1029	9.90
8350	14879	1027	9.73	8518	14878	1024	9.58	8687	14880	1021	9.43
8854	14887	1020	9.27	9022	14893	1019	9.08	9190	14900	1018	8.83
9358	14906	1016	8.54	9517	14908	1016	8.28	9671	14906	1017	8.07
9824	14904	1017	7.87	9978	14902	1018	7.68	10131	14901	1018	7.50
10285	14899	1019	7.33	10482	14897	1026	7.17	10708	14894	1037	7.03
N2500				5657	15452	946	6.61	5829	15443	944	7.19
				6002	15435	943	7.77	6174	15426	941	8.15
6347	15417	939	8.61	6520	15408	937	9.15	6692	15400	936	9.76
6864	15399	936	10.40	7035	15403	938	10.94	7095	15404	939	11.05
7207	15406	940	10.98	7378	15410	942	10.80	7550	15413	944	10.52
7721	15416	946	10.20	7893	15420	948	9.91	8064	15423	950	9.65
8236	15427	952	9.43	8407	15430	954	9.23	8584	15428	953	9.04
8764	15424	951	8.86	8943	15420	950	8.67	9122	15417	948	8.45
9302	15413	947	8.20	9475	15409	945	7.95	9636	15407	940	7.71
9801	15407	937	7.48	9977	15412	941	7.26	10154	15416	944	7.05
10330	15420	948	6.85	10507	15425	951	6.66	10683	15429	955	6.47

x	y	z	t	x	y	z	t	x	y	z	t
N3000				5222	15839	998	5.56	5379	15836	1008	6.05
				5537	15832	1019	6.61	5695	15828	1030	7.28
5852	15825	1041	8.03	6024	15833	1042	8.68	6200	15843	1040	9.14
6375	15854	1039	9.56	6550	15865	1037	9.96	6725	15876	1036	10.34
6901	15886	1034	10.70	7076	15897	1033	11.03	7227	15896	1030	11.23
7341	15896	1027	11.32	7379	15896	1026	11.23	7530	15895	1023	10.96
7682	15895	1020	10.76	7833	15894	1016	10.58	7984	15894	1013	10.44
8136	15893	1010	10.28	8278	15891	1008	10.07	8409	15885	1006	9.82
8540	15880	1005	9.56	8671	15874	1004	9.31	8802	15883	1005	9.08
8933	15895	1005	8.89	9065	15907	1006	8.78	9196	15919	1007	8.73
9327	15931	1008	8.71	9459	15943	1009	8.70	9590	15955	1010	8.64
9721	15967	1010	8.49	9868	15975	1011	8.28				
N3500				4841	16449	969	5.66	5021	16442	966	6.06
				5201	16437	967	6.49	5380	16432	967	7.06
5559	16427	967	7.75	5738	16422	968	8.09	5918	16417	968	8.31
6097	16412	968	8.51	6276	16406	969	8.70	6455	16401	969	8.90
6629	16399	968	9.17	6799	16400	965	9.55	6968	16401	963	10.09
7138	16401	961	10.67	7308	16402	959	11.13	7392	16402	958	11.29
7477	16403	956	11.22	7655	16405	956	11.04	7834	16407	957	10.79
8014	16409	957	10.46	8193	16410	957	10.06	8373	16412	958	9.61
8552	16414	958	9.20	8732	16413	956	8.91	8912	16410	954	8.73
9092	16406	951	8.65	9262	16405	950	8.59	9425	16405	950	8.53
9588	16405	950	8.44	9750	16405	950	8.29	9913	16406	951	8.06
10076	16406	951	7.77	10239	16406	951	7.44	10402	16406	951	7.08
10565	16406	951	6.70								
N4000				4755	16880	1049	6.59	4909	16873	1050	7.00
				5064	16865	1051	7.29	5219	16858	1051	7.52
5374	16851	1052	7.73	5528	16844	1053	7.93	5684	16844	1051	8.13
5841	16844	1049	8.33	5997	16844	1047	8.55	6153	16845	1045	8.79
6309	16845	1043	9.06	6466	16845	1041	9.36	6622	16845	1038	9.67
6778	16845	1036	10.01	6934	16846	1034	10.38	7090	16846	1032	10.79
7247	16846	1030	11.25	7404	16846	1028	11.73	7558	16850	1025	12.25
7585	16851	1024	12.20	7747	16856	1021	11.84	7890	16860	1020	11.46
8033	16864	1018	11.06	8176	16868	1017	10.64	8319	16872	1016	10.25
8462	16876	1014	9.90	8605	16880	1013	9.61	8748	16884	1011	9.37
8891	16888	1010	9.17	9049	16890	1009	8.99	9230	16891	1009	8.83
9411	16891	1008	8.67	9592	16892	1008	8.52	9773	16893	1008	8.37
9954	16893	1008	8.23	10135	16894	1008	8.09	10316	16894	1007	7.94
10497	16895	1007	7.78	10678	16896	1007	7.60	10859	16896	1007	7.41
11040	16897	1006	7.20								
N4500				4720	17469	1002	7.27	4901	17457	1000	7.76
				5083	17444	999	7.98	5265	17431	998	7.96
5447	17418	996	7.83	5628	17406	995	7.84	5810	17395	995	8.03
5986	17398	998	8.31	6163	17400	1002	8.62	6340	17402	1006	8.94
6517	17404	1009	9.26	6693	17407	1013	9.60	6870	17409	1017	9.97
7044	17421	1016	10.41	7218	17434	1014	10.90	7392	17446	1013	11.54
7479	17452	1012	11.79	7566	17459	1011	11.74	7740	17472	1010	11.49
7916	17476	1009	11.15	8098	17466	1007	10.73	8279	17456	1006	10.25
8460	17446	1005	9.74	8641	17436	1004	9.22	8822	17426	1003	8.75
9003	17422	1003	8.41	9184	17431	1005	8.25	9364	17441	1007	8.17
9544	17450	1009	8.07	9725	17459	1012	7.91	9902	17463	1016	7.68
10076	17457	1024	7.36	10250	17452	1032	6.94				
N5000				4629	17872	1004	5.64	4791	17870	1007	6.04
				4953	17868	1010	6.60	5115	17866	1013	7.19
5274	17865	1015	7.67	5426	17870	1017	7.89	5578	17874	1019	8.10
5730	17878	1020	8.32	5882	17883	1022	8.59	6035	17887	1024	8.90
6187	17892	1025	9.21	6339	17896	1027	9.51	6491	17900	1028	9.80
6643	17905	1030	10.08	6805	17890	1032	10.35	6966	17873	1033	10.66
7128	17857	1035	11.04	7292	17860	1035	11.55	7416	17866	1035	12.00
7458	17868	1035	11.95	7624	17876	1034	11.72	7789	17884	1034	11.48
7955	17892	1034	11.21	8120	17900	1034	10.92	8286	17908	1033	10.63
8452	17916	1033	10.33	8600	17915	1032	10.02	8742	17911	1030	9.69
8884	17908	1028	9.33	9026	17904	1027	8.93	9188	17904	1023	8.50
9366	17907	1019	8.04	9545	17910	1014	7.57	9723	17913	1009	6.95
9902	17916	1005	6.46	10080	17919	1000	6.10				

x	y	z	t	x	y	z	t	x	y	z	t
N5500				4816	18404	1008	5.38	5007	18406	1016	5.91
				5198	18409	1024	6.63	5390	18411	1032	7.51
5580	18413	1039	8.12	5752	18418	1040	8.47	5924	18424	1041	8.77
6095	18429	1042	9.03	6267	18434	1043	9.28	6446	18432	1042	9.55
6631	18420	1041	9.93	6817	18409	1040	10.47	7003	18398	1039	11.13
7188	18386	1038	11.82	7346	18377	1036	12.41	7374	18375	1036	12.33
7560	18363	1035	11.92	7737	18363	1036	11.64	7911	18366	1037	11.36
8086	18368	1038	10.85	8261	18371	1039	10.31	8435	18373	1040	9.92
8610	18376	1041	9.62	8785	18379	1042	9.32	8959	18383	1043	8.98
9134	18386	1043	8.52	9309	18390	1044	7.94	9483	18394	1044	7.22
9658	18398	1045	6.36								
N6000				5639	18895	1054	8.46	5812	18892	1051	8.85
				5987	18891	1048	9.12	6162	18891	1044	9.35
6337	18890	1041	9.61	6512	18890	1037	9.99	6687	18890	1033	10.44
6862	18889	1030	10.97	7037	18889	1026	11.64	7212	18888	1023	11.92
7264	18887	1022	11.98	7387	18884	1021	11.85	7565	18869	1022	11.62
7742	18854	1025	11.35	7913	18844	1026	11.05	8065	18850	1025	10.69
8216	18856	1023	10.24	8368	18862	1022	9.70	8519	18868	1021	9.18
8671	18874	1020	8.77	8823	18880	1019	8.45	8974	18886	1017	8.15
9126	18891	1016	7.86	9281	18897	1015	7.38				
W500				9281	18897	1015	7.38	9515	13639	1052	7.11
				9510	13778	1042	7.32	9506	13917	1033	7.52
9505	14054	1032	7.71	9504	14191	1032	7.89	9503	14328	1031	8.05
9503	14466	1031	8.17	9502	14603	1031	8.21	9501	14740	1030	8.28
9505	14876	1032	8.39	9509	15011	1033	8.44	9513	15146	1035	8.47
9517	15281	1037	8.50	9521	15417	1039	8.53	9525	15552	1041	8.58
9529	15685	1040	8.65	9533	15817	1038	8.74	9538	15949	1036	8.84
9542	16081	1034	8.94	9546	16213	1033	9.00	9550	16345	1031	9.02
9549	16479	1031	9.00	9544	16616	1033	8.95	9538	16752	1036	8.87
9533	16889	1038	8.76	9527	17025	1040	8.63	9523	17161	1042	8.49
9534	17291	1040	8.35	9545	17421	1038	8.26	9557	17550	1036	8.25
9568	17680	1034	8.18	9579	17809	1032	7.87				
W1000				8981	13978	1056	8.22	8984	14111	1058	8.20
				8987	14243	1060	8.21	8990	14376	1062	8.30
8993	14508	1064	8.50	8996	14640	1066	8.88	9002	14773	1066	9.22
9012	14905	1064	9.39	9022	15038	1062	9.41	9032	15170	1060	9.36
9042	15303	1058	9.30	9052	15435	1056	9.25	9046	15571	1053	9.20
9039	15707	1051	9.16	9032	15843	1048	9.11	9026	15979	1046	9.04
9019	16115	1043	8.98	9013	16251	1040	9.04	9017	16384	1041	9.22
9022	16515	1042	9.31	9028	16647	1043	9.32	9033	16779	1045	9.30
9038	16911	1046	9.24	9044	17043	1047	9.05	9049	17175	1048	8.81
9044	17310	1049	8.65	9039	17445	1049	8.65	9034	17579	1050	8.75
9029	17714	1050	8.92	9024	17849	1051	9.08	9018	17981	1052	9.15
9010	18111	1054	9.16	9003	18240	1055	9.11	8995	18370	1057	9.01
8988	18500	1059	8.85	8980	18629	1060	8.68	8982	18769	1062	8.52
8989	18913	1064	8.40	8995	19058	1066	8.32	9002	19202	1067	8.27
9008	19346	1069	8.23	9013	19489	1071	8.20	9017	19628	1072	8.18
9021	19768	1073	8.16	9025	19907	1075	8.14	9029	20046	1076	8.13
9033	20186	1078	8.12								
W2000				7997	13427	1138	9.91	7998	13558	1123	9.76
				7998	13690	1108	9.63	7999	13821	1093	9.53
8000	13952	1078	9.45	8000	14083	1063	9.39	8001	14215	1048	9.36
8003	14349	1043	9.38	8007	14485	1043	9.51	8010	14622	1043	9.76
8014	14758	1043	10.01	8017	14894	1043	10.19	8020	15030	1043	10.24
8024	15166	1043	10.27	8018	15302	1041	10.30	8011	15438	1039	10.33
8004	15574	1037	10.37	7997	15709	1035	10.44	7991	15845	1033	10.52
7988	15984	1033	10.63	7989	16126	1034	10.75	7991	16268	1036	10.88
7992	16410	1038	11.01	7994	16553	1039	11.14	7995	16695	1041	11.24
7996	16832	1043	11.30	7997	16965	1044	11.33	7998	17097	1045	11.33
7999	17229	1047	11.31	8000	17361	1048	11.28	8001	17493	1050	11.25
7994	17632	1051	11.24	7983	17774	1052	11.26	7973	17915	1053	11.30
7962	18056	1054	11.36	7952	18198	1055	11.42	7941	18339	1057	11.42
7943	18484	1059	11.38	7952	18630	1061	11.32	7962	18776	1064	11.25
7971	18922	1067	11.17	7981	19068	1069	11.09	7986	19214	1071	11.01
7990	19360	1073	10.93	7994	19506	1075	10.85	7998	19652	1076	10.78
8002	19799	1078	10.71	8007	19945	1079	10.64				

x	y	z	t	x	y	z	t	x	y	z	t
W2500				7511	13499	1030	9.58	7514	13642	1031	9.67
				7516	13784	1031	9.74	7518	13926	1031	9.79
7521	14069	1032	9.83	7521	14208	1032	9.88	7518	14343	1033	9.97
7515	14478	1033	10.20	7513	14613	1034	10.58	7510	14748	1034	10.92
7507	14883	1035	11.14	7501	15017	1034	11.26	7496	15150	1033	11.30
7490	15283	1033	11.29	7484	15417	1032	11.24	7478	15550	1031	11.16
7472	15684	1030	11.09	7483	15820	1029	11.05	7499	15956	1028	11.08
7514	16093	1027	11.19	7530	16230	1027	11.36	7546	16367	1026	11.57
7556	16504	1026	11.81	7556	16641	1027	12.06	7556	16778	1029	12.24
7555	16916	1030	12.27	7555	17053	1032	12.19	7555	17190	1034	12.09
7553	17328	1035	12.00	7546	17466	1036	11.93	7539	17604	1037	11.88
7532	17742	1037	11.86	7525	17881	1038	11.88	7517	18019	1039	11.95
7510	18157	1040	12.02	7507	18297	1040	12.06	7511	18438	1040	12.04
7514	18579	1040	11.98	7518	18720	1040	11.90	7521	18862	1040	11.81
7525	19003	1040	11.73	7529	19143	1040	11.66	7535	19281	1040	11.60
7541	19418	1040	11.54	7547	19556	1040	11.49	7553	19693	1040	11.45
7559	19831	1040	11.42	7564	19968	1040	11.40				
W3000				6997	13222	1070	10.42	6996	13361	1070	10.63
				6995	13501	1070	10.68	6994	13641	1070	10.66
6993	13781	1070	10.61	6992	13920	1070	10.57	6992	14063	1070	10.57
6995	14209	1071	10.61	6998	14356	1072	10.71	7001	14502	1073	10.85
7004	14648	1074	11.00	7007	14792	1075	11.14	7006	14919	1074	11.28
7005	15046	1073	11.43	7005	15173	1073	11.58	7004	15300	1072	11.69
7003	15426	1071	11.69	7002	15553	1070	11.57	6998	15686	1069	11.40
6993	15820	1068	11.20	6987	15955	1068	11.03	6982	16089	1067	10.91
6976	16223	1066	10.80	6973	16358	1065	10.73	6976	16495	1064	10.71
6979	16633	1063	10.72	6983	16770	1063	10.72	6986	16907	1062	10.69
6990	17044	1061	10.64	6993	17181	1060	10.58	6995	17320	1059	10.54
6995	17461	1056	10.57	6995	17602	1053	10.66	6996	17744	1050	10.75
6996	17885	1047	10.84	6996	18026	1044	10.92	6996	18168	1040	10.99
6994	18305	1041	11.06	6992	18442	1042	11.14	6990	18579	1043	11.26
6988	18716	1044	11.40	6986	18852	1044	11.54	6984	18989	1045	11.66
6982	19126	1046	11.77	6980	19263	1047	11.88	6977	19400	1048	11.99
6975	19537	1049	12.10	6973	19673	1050	12.20				
W3500				6494	12762	1113	9.17	6500	12933	1097	9.40
				6506	13104	1080	9.81	6513	13275	1063	10.21
6519	13446	1047	10.46	6528	13619	1035	10.42	6541	13797	1033	10.30
6555	13974	1032	10.10	6568	14151	1030	9.87	6579	14329	1028	9.65
6574	14512	1028	9.57	6569	14696	1029	9.54	6563	14879	1029	9.54
6558	15062	1030	9.56	6553	15245	1030	9.59	6547	15428	1031	9.66
6542	15611	1031	9.78	6536	15791	1032	9.91	6531	15969	1033	9.84
6525	16147	1035	9.63	6519	16326	1036	9.47	6513	16504	1037	9.41
6507	16683	1038	9.41	6513	16864	1038	9.42	6527	17046	1037	9.43
6540	17229	1035	9.44	6554	17412	1034	9.49	6567	17594	1032	9.64
6581	17777	1031	9.87	6585	17955	1031	10.00	6583	18129	1033	9.90
6581	18303	1035	9.75	6579	18477	1036	9.74	6577	18652	1038	9.92
6573	18831	1039	10.12	6568	19014	1039	10.30	6563	19198	1039	10.46
6558	19381	1039	10.61	6553	19564	1040	10.74	6548	19748	1040	10.84
6543	19931	1040	10.94								
W4000				6165	12854	1066	8.97	6163	13038	1061	8.77
				6160	13222	1057	9.12	6158	13406	1052	9.56
6155	13590	1048	9.75	6156	13776	1044	9.75	6161	13965	1043	9.54
6165	14153	1042	9.12	6170	14342	1041	8.74	6175	14530	1039	8.63
6169	14713	1039	8.61	6159	14892	1038	8.61	6149	15072	1038	8.63
6139	15251	1038	8.66	6128	15431	1037	8.71	6118	15610	1037	8.76
6108	15789	1036	8.83	6096	15969	1036	8.89	6069	16149	1035	8.93
6042	16328	1033	8.94	6022	16503	1034	8.87	6004	16675	1035	8.65
5987	16846	1037	8.47	5969	17018	1038	8.40	5952	17190	1039	8.41
5934	17362	1041	8.48	5917	17534	1042	8.60	5899	17706	1044	8.71
5895	17888	1046	8.78	5899	18075	1050	8.81	5903	18262	1054	8.84
5907	18449	1058	8.88	5909	18631	1061	8.94	5909	18806	1062	9.02
5910	18981	1064	9.11	5910	19156	1066	9.21	5910	19331	1067	9.31
5911	19506	1069	9.41	5911	19685	1071	9.51	5913	19873	1072	9.61
5915	20061	1074	9.71								